Assessing Aquitard Integrity:

the Newmarket Till (Southern Ontario)

Ramina Rashtchi

Thesis submitted to the University of Ottawa
in partial Fulfillment of the requirements for the
Master of Earth and Environmental Sciences

Department of Earth and Environmental Sciences
Faculty of Science
University of Ottawa

Abstract

The Newmarket Till is a regional aquitard in southern Ontario that overlies the Illinoian to Middle Wisconsinan Lower Sediments and is overlain by the Oak Ridges Moraine (ORM). Geological investigations have mapped the distribution of the till and it is understood that erosional channels, subsequently infilled with fluvial material, breach the till and may create enhanced hydraulic connection between overlying and underlying aquifers. However, little is known about the protective capability of the Newmarket Till where it is intact. This study used natural tracers to assess the extent of transport in the aquitard-aquifer system. Stable isotopes of water ($\delta^{18}O$ and $\delta^{2}H$) showed a depletion trend versus depth. In the Newmarket Till most of the samples had isotope ratios similar to meteoric water data from the nearest location (Egbert, ON). The depleted values of $\delta^{18}O$ in the Thorncliffe Formation suggest a remnant signature of early-Holocene precipitation (-16‰ at the depth of 60 m).

Elevated levels of NO_3^- and Cl^- were detected near the surface and because of the low permeability aquitard (Newmarket Till), they could not migrate to depth. Total extractable ammonium concentrations are ranging from 4.09 ppm from near the surface to 60 ppm in the lowest part of the Newmarket and then gradually increase to 514 ppm in the bottom of the Thorncliffe Formation. The combination of high NH_4^+ values and organic carbon content in the Thorncliffe Formation suggests a natural source from mineralization of organic N. The fractionation which happened between $\delta^{15}N$-sediment and $\delta^{15}N$-NH_4 may have three explanations: (1) lighter isotopes diffuse faster than heavier ones, so the higher rate of diffusion can cause fractionation; (2) heavier isotopes partition to exchange sites, causing fractionation along the transport pathway; (3) dissociation of NH_4^+ to NH_3 under anaerobic condition.

Positive values for $\delta^{13}C$ in groundwater in the Thorncliffe Formation are likely due to i) a contribution of carbonate mineral dissolution, and ii) methanogenesis - the Archea favor the lighter isotope of C (^{12}C). Methanogenesis therefore enriches the $\delta^{13}C$-DIC was enriched; however, the $\delta^{13}C$ in dissolved organic carbon (DOC) is depleted.

These geochemical characteristics demonstrate a long residence time for the porewater in the system and indicate that the Newmarket till inhibits recharge of recent precipitation, thereby providing protection to the underlying aquifers from surface-derived contaminants.

Acknowledgments

The past few years of this thesis marks significant scientific, professional and personal growth in my life. I am thankful to have met and learned from so many incredible people and am grateful for the time, knowledge, support and enthusiasm they contributed along the way.

Foremost, I thank my supervisor Tom Al, who has been instrumental to the success of this project and my personal development. Throughout my thesis his patience, knowledge, curiosity and positivity has been invaluable. He has been supportive of me trying new techniques and pushing me to chase my own scientific curiosity. Thank you for helping with the knowledge and confidence needed to grow as a scientist.

I am grateful to Hazen Russell and Bruce Kjarsgaard from the GSC for their support and advice throughout the development of this project.

This project would not have been possible without the many members of the uOttawa staff that helped with various aspects including Nimal DeSilva, Smita Mohanty, Monika Wilk, Paul Middlestead, Anthony Lapp, Wendy Abdi, Kerry Klassen, Patricia Wickham, Sarah Murseli and Barbara Fransisco.

Thank you, members of Tom's research group, all of you have contributed in some way to both the project and my professional growth. I would specifically like to thank Magda, Golrokh, Carla, Dominique, Birendra, Simon and Dania; this project would not have been possible without your encouragement, knowledge, motivation and enthusiasm.

I am deeply grateful to my former supervisor, Jack Cornett, for his kind assistance and patience with me. He supported me morally and materially at difficult moments and his family always made me feel at home.

A special appreciation for Soroush Shahryari Fard who found time in a rather busy schedule for proof reading.

Thank you to my family, for their endless encouragement and support along this journey.

Finally, I sincerely thank my husband Hamed, who listened and discussed ideas about this thesis with me on many occasions.

Table of Contents

List of Figures

List of Tables

List of abbreviations

AMS	Accelerator Mass Spectrometry
DIC	*Dissolved Inorganic Carbon*
DOC	*Dissolved Organic Carbon*
EA	Elemental Analyzer
GSC	Geological Survey of Canada
GTA	Greater Toronto Area
HVE	High Voltage Engineering
IC	Ion Chromatography
ICP-MS	Inductively coupled plasma mass spectrometry
IRMS	Isotope ratio Mass Spectrometer
LGR	Los Gatos Research
ORM	Oak Ridge Moraine
PDB	Pee Dee Belemnite
S/L	*Solid-Liquid Ratio*
SOC	*Solid Organic Carbon*
TIWA	Triple Isotope Water Analyzer
VD	Vacuum Distillation
VSMOW	Vienna Standard Mean Ocean Water

Chapter 1 - Introduction

As demand for groundwater resources increases and management of the resources becomes a critical issue, aquitards are one of the most important components of groundwater flow systems. Aquifers are normally the focus of attention because they are the source of water supply and are the zones where large contaminant plumes develop. At waste disposal or industrial sites, however, aquitards are often as important as the aquifers (Cherry, 1990). The problems of monitoring aquitards are much different than those of aquifers. Aquitards control recharge and contaminant transport to adjacent aquifers (Gerber, 1999). Figure 1.1 displays an aquitard-aquifer system. Aquitards do not provide wells with quantities of water, but generally determine flow paths and represent storage units for groundwater (Cherry et al., 2004). Aquitards are low hydraulic conductivity geologic deposits that help protect groundwater resources from contamination by impeding downward flow. Aquitards can decrease the susceptibility of underlying groundwater to contamination by increasing both time of travel and the flow path distance from contaminated overlying groundwater sources. Assessment of the protection capacity of aquitards depends on the contaminant characteristics and hydrogeologic characteristics. The degree to which an aquitard protects underlying aquifers depends on the hydraulic conductivity (K) which is largely controlled by the type of geologic material (Gerber, 1999). The bulk K reflects the geologic matrix material and Hendry (1988) indicates that aquitard values are typically $< 1 \times 10^{-10}$ m/s, resulting in groundwater flow rates of 1 m per 1000 years or lower (Hendry 1988; Remenda et al., 1996; Hendry and Wassenaar, 1999). Under these conditions, solute transport is, in general, dominated by molecular diffusion (Hendry and Wassenaar, 1999).

The second parameter that can influence the degree of aquitard protection should be the thickness of the aquitard. In general, aquitards that are tens of meters thick protect better than thinner, low-permeability zones.

Attenuation and retardation can affect contaminant transport within an aquitard. Bulk density, pH, mineral content, the fraction of organic carbon, and cation exchange capacity are some of the aquitard and porewater characteristics that should be considered for evaluation of the attenuation and retardation through the aquitard (Bradbury et al., 2006; Cherry et al., 2006).

The mobility of contaminants through aquitards depends on physical or chemical characteristics of contaminants. Contaminants in groundwater can be present as a dissolved (soluble) or free liquid phase (insoluble). Movement of the dissolved phase is mostly governed by advection-dispersion mechanisms and transport is in the direction of groundwater flow (Huling and Weaver, 1991).

The focus of this research is on a borehole located north of Pickering, ON and south of the Oak Ridge Moraine (ORM). The ORM is one of the most significant landforms in southern Ontario. It is a recharge area for aquifers supplying the Greater Toronto Area (GTA) supplying water to more than 60,000 wells (Sharpe et al., 2007). The sediments located in the ORM area are divided into the Lower Sediments, the Newmarket Till, the ORM sediments and the Halton Till (Sharpe et al., 2007).

During the Late Wisconsinan, the Newmarket Till (also referred to as the Northern Till) was deposited by the Laurentide ice sheet. It is a regionally extensive confining unit and separates the upper aquifer systems associated with the ORM sediments from the lower aquifer systems that occur within deposits of the Scarborough and Thorncliffe Formations (Wexler et al., 2004 ; Kassenaar and Wexler 2006).

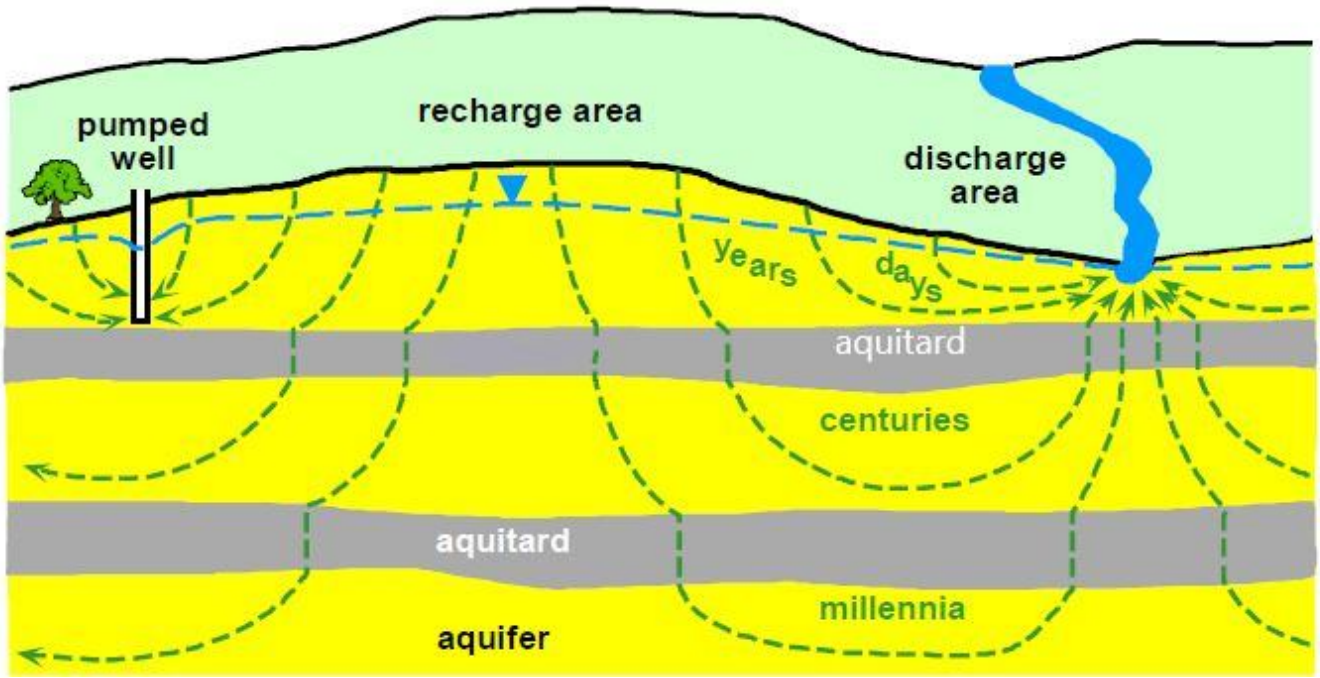

Fig. 1.1. Schematic diagram shows groundwater flow lines in aquitards and aquifers system modified after (Toth, 1995)

1.1. Objectives

The overall purpose of this research was to assess the degree to which the Newmarket Till provides protection for underlying aquifers. To address this issue, four specific objectives were defined:

- To collect vertical geochemical profiles from the aquitard porewater
- To understand the origin of solute and isotope profiles
- To understand the redox conditions in the aquitard
- To investigate the mechanisms of solute transport

1.2. Thesis Structure

This thesis has been written in an article format, where the body of the thesis consists of 1 independent paper (chapter two) with the intention that it will be submitted to a scientific journal for publication.

Chapter two describes vertical geochemical profiles that were collected to assess the degree to which the Newmarket Till provides protection for underlying aquifers. Naturally occurring ionic solutes (Cl and NO_3), as well as stable ($\delta^{18}O$ and $\delta^{2}H$) and radiogenic isotopes (^{14}C) that are tracers of water and solute transport, were used. Furthermore, analyses of aqueous methane (CH_4), ammonium (NH_4^+), dissolved inorganic carbon (DIC) and dissolved organic carbon (DOC) were used to characterize the redox conditions.

Chapter 3 provides a brief summary and conclusions in the context of the whole project.

1.3. References

Bradbury, K.R., Gotkowitz, M.B., Hart, D.J., Eaton, T.T., Cherry, J.A., Parker, B.L., and Borchardt, M.A., 2006, Contaminant transport through aquitards: technical guidance for aquitard assessment: Publication 91133b, American Water Works Association Research Foundation,.

Bremner, J.M., and Keeney, D.R., 1966, Determination and isotope-ratio analysis of different forms of nitrogen in soils: 3. exchangeable ammonium, nitrate, and nitrite by extraction-distillation methods 1: Soil Science Society of America Journal, v. 30, p. 577–582.

Cherry, J., 1990, Groundwater Monitoring: Some Deficiencies and Opportunities. Hazardous Waste Site Investigationns; Towards Better decision: Proceedings of 10th ORNL Life sciences symposium Gatlinberg, TN,.

Cherry, J.A., Parker, B.L., Bradbury, K.R., Eaton, T.T., Gotkowitz, M.G., Hart, D.J., and Borchardt, M.A., 2004, Role of aquitards in the protection of aquifers from contamination: a “state of the science” report: Awwa Research Foundation, Denver, Colo,.

Du, Y., Ma, T., Deng, Y., Shen, S., and Lu, Z., 2017, Sources and fate of high levels of ammonium in surface water and shallow groundwater of the Jianghan Plain, Central China: Environmental Science: Processes & Impacts, v. 19, p. 161–172.

Gerber, R., 1999, Hydrogeologic behaviour of the Northern till aquitard near Toronto, Ontario: National Library of Canada= Bibliothèque nationale du Canada.

Gerber, R.E., and Howard, K.W.F., 1996, Evidence for recent groundwater flow through Late Wisconsinan till near Toronto, Ontario: Canadian Geotechnical Journal, v. 33, p. 538–555.

Gerber, R.E., and Howard, K., 2000, Recharge through a regional till aquitard: Three-dimensional flow model water balance approach: Groundwater, v. 38, p. 410–422.

Haynes, R., 2012, Mineral nitrogen in the plant-soil system: Elsevier.

Hendry, M.J., 1988, Hydrogeology of clay till in a prairie region of Canada: Groundwater, v. 26, p. 607–614.

Hendry, M.J., and Wassenaar, L.I., 1999, Implications of the distribution of $δ$D in pore waters for groundwater flow and the timing of geologic events in a thick aquitard system: Water Resources Research, v. 35, p. 1751–1760.

Hoefs, J., 2009, Stable isotope geochemistry: Springer, v. 285.

Huling, S.G., and Weaver, J.W., 1991, Ground water issue: dense nonaqueous phase liquids: US Environmental Protection Agency.

Kassenaar, J.D.C., and Wexler, E.J., 2006, Groundwater modelling of the Oak Ridges Moraine area: CAMC-YPDT Technical Report,.

Lindenbaum, J., 2012, Identification of sources of ammonium in groundwater using stable nitrogen and boron isotopes in Nam Du, Hanoi: Dissertations in Geology at Lund University.

Li, L., Lollar, B.S., Li, H., Wortmann, U.G., and Lacrampe-Couloume, G., 2012, Ammonium stability and nitrogen isotope fractionations for NH4+--NH3 (aq)--NH3 (gas) systems at 20--70° C and pH of 2--13: applications to habitability and nitrogen cycling in low-temperature hydrothermal systems: Geochimica et Cosmochimica Acta, v. 84, p. 280–296.

Remenda, V.H., der Kamp, G., and Cherry, J.A., 1996, Use of vertical profiles of $δ$18O to constrain estimates of hydraulic conductivity in a thick, unfractured aquitard: Water Resources Research, v. 32, p. 2979–2987.

Sharpe, D.R., Russell, H.A.J., and Logan, C., 2007, A 3-dimensional geological model of the Oak Ridges Moraine area, Ontario, Canada: Journal of Maps, v. 3, p. 239–253.

Toth, J., 1995, Hydraulic continuity in large sedimentary basins: Hydrogeology Journal, v. 3, p. 4–16.

Wexler, E., Holysh, S., Kassenaar, D., and Gerber, R., 2004, Regional and Sub-Regional Groundwater Flow Modelling, Oak Ridges Moraine Area of Southern Ontario.

Chapter 2 – Hydrogeochemistry of a Quaternary Aquifer-Aquitard System; Southern Ontario

2.0. Abstract

The Newmarket Till is a regional aquitard in southern Ontario that overlies the Illinoian to Middle Wisconsinan Lower Sediments (includes the Thorncliffe Formation) and is overlain by the Oak Ridges Moraine (ORM). This study used natural tracers to assess the transport mechanisms in the aquitard-aquifer system. Stable isotopes of water ($\delta^{18}O$ and $\delta^{2}H$) showed a depletion trend versus depth. In the upper portion of the Newmarket Till most of the samples had isotopic ratios similar to meteoric water from the nearest location (Egbert, ON). The depleted values of $\delta^{18}O$ in the lower Newmarket till and the Thorncliffe Formation showed a signature of early-Holocene times (-16‰) at the depth of 60 m. Relatively high levels of NO_3^- and Cl^- have been detected near the surface and because of the low permeability aquitard (Newmarket Till) they could not migrate downward. Concentrations of total extractable ammonium (NH_4^+; includes mass in the porewater and on ion exchange sites) range from 4.09 ppm in the Newmarket till, and increase to 515 ppm near the base of the Thorncliffe Formation. The combination of high NH_4^+ values and organic carbon content in the Thorncliffe Formation suggests a natural source from mineralization of organic N. Fractionation which happened between $\delta^{15}N$-sediment and $\delta^{15}N$-NH_4 may have three explanations: (1) variable diffusion rate for ^{14}N versus ^{15}N; (2) heavier isotopes (^{15}N) are preferentially partitioned into the exchange site; (3) dissociation of NH_4^+ to NH_3 under anaerobic condition and degassing of NH_3 from the system. Two possible explanations for an increasing trend of $\delta^{13}C$ in dissolved inorganic carbon (DIC) versus depth could be identified: (1) the positive value of $\delta^{13}C$ in the Thorncliffe Formation was a result of equilibration of $\delta^{13}C$ with calcite dissolution; (2) methanogenesis reaction. During biologically mediated methanogenesis reactions, the micro-organisms preferentially select lighter

isotope of C (^{12}C) leading to enrichment of ^{13}C in the residual DIC and formation of CH_4 that has a depleted $\delta^{13}C$ signature.

These geochemical characteristics demonstrate a long residence time for the porewater in the system and indicate that the Newmarket till inhibits recharge of recent precipitation, thereby providing protection to the underlying aquifers from surface-derived contaminants.

2.1. Introduction

Aquitards are important components of groundwater systems, but they are commonly poorly understood because characterization methods are more challenging than for aquifers. Recharge and contaminant transport to underlying aquifers are controlled by aquitards. Assessment of the protection capacity of aquitards depends on the contaminant type, magnitude and direction of groundwater flow and the geologic setting (Cherry et al., 2004). Industry and government are both very interested in aquitard systems because of their potential use for geological storage of wastes and for their role as a protective cover for regional aquifer systems (Hendry and Wassenaar, 1999). Quantified management of groundwater resources has become a critical issue as the demand for groundwater increases. Vertical leakage through tills is an important component of recharge, and transport of anthropogenic contamination into underlying aquifers is a concern (Gerber, 1999).

Measuring vertical leakage can be very difficult because of spatial variability in hydraulic conductivity (K) and hydraulic gradients. Knowledge of the bulk K of regional aquitards can be used to estimate vertical leakage (Gerber and Howard, 2000). The bulk K reflects the geologic matrix material and Hendry (1988) indicates that aquitard values are typically $< 1 \times 10^{-10}$ m/s, resulting in groundwater flow rates of 1 m per 1000 years or lower (Hendry, 1988; Remenda et al., 1994, 1996; Wassenaar and Hendry, 1999). Under these conditions, solute transport is, in general, dominated by molecular diffusion (Hendry and Wassenaar, 1999).

In past decades, it was not uncommon that the effect of diffusion in porous media was disregarded in some solute transport studies. Schwartz et al., (1983), Smith and Schwartz (1984), and Cacas et al. (1990) are examples of studies that have considered groundwater flow and solute transport in discrete fracture networks, but without consideration of solute diffusion. More recently, many studies have shown the influence of solute diffusion on transport. For example Desaulniers et al., (1981), Desaulniers et al. (1986), Desaulniers and Cherry (1989), Remenda et al., (1994), Remenda et al. (1996), and Hendry and Wassenaar (1999) indicate that diffusion is an important transport process in aquitards. Desaulniers et al. (1981) and Desaulniers and Cherry (1989) focused on using natural tracer profiles for clay deposits in southwestern Ontario and southern Quebec, respectively. They used oxygen and hydrogen isotopes in water to estimate advection/diffusion rates and concluded that depleted values for $\delta^{18}O$ can be used as a signature for water of Pleistocene origin. These and other studies used $\delta^{18}O$ and $\delta^{2}H$ to show that molecular diffusion is the dominant transport mechanism in several aquitards. They rely on the fact that water in glacially deposited clay sediments has values of $\delta^{18}O$ and $\delta^{2}H$ that are depleted relative to modern precipitation. Desaulniers and Cherry (1989) also used analytical models for advection and diffusion of major ions to determine that a thick deposit of Champlain Sea clay near Montreal is unfractured and that molecular diffusion is the dominant solute transport mechanism. Their work and many subsequent studies have determined that natural tracers can be used to evaluate the hydro-chemical behavior of both fractured and non-fractured clayey aquitards. Remenda et al. (1996) obtained similar conclusions for $\delta^{18}O$ and $\delta^{2}H$ profiles for Quaternary tills in Saskatchewan, Canada. They used the vertical profiles of $\delta^{18}O$ to estimate the hydraulic conductivity in thick unfractured aquitards. Gerber and Howard (1996) also used isotopic data ($\delta^{18}O$, $\delta^{2}H$ and ^{3}H) in their studies of the Northern Till (Newmarket Till) and determined that preferential pathways exist to deliver young (post-1952) water to various depths in the aquitard. In addition, Gerber and Howard (2000) concluded that for the glacial till units in Ontario, the regional

permeability is several orders of magnitude larger than the matrix permeability. Hendry et al. (2004) used a high-resolution 1-D profile for $\delta^{18}O$ and $\delta^{2}H$ to identify three hydrogeologic zones in a thick till aquitard system in Saskatchewan, Canada. In the lower zone of the till, the curved shape of the isotope profile suggests that molecular diffusion controls solute transport. In the intermediate zone, the lack of vertical variability suggests that a system of interconnected vertical fractures and lateral sand layers regulated the solute transport in this zone. A sand layer with high hydraulic conductivity (K) was controlled the transport in the upper hydrogeological zone.

The principal objective of this study is to use vertical geochemical profiles to assess the degree to which the Newmarket Till (Sothern Ontario) provides protection for underlying aquifers. We aim to understand the origin of solute and isotope profiles, the redox conditions and mechanisms of solute transport.

2.2. Geology

This research focuses on a borehole located north of Pickering, ON, about 45 km north-east of Toronto (Fig. 2.1). This area is located the south of the Oak Ridge Moraine (ORM). The ORM is one of the most significant landforms in southern Ontario. It is a recharge area for aquifers supplying the Greater Toronto Area (GTA) supplying water to more than 60,000 wells (Sharpe et al., 2007). The sediments located in the ORM area are divided into the Lower Sediments, the Newmarket Till, the ORM sediments and the Halton Till (Sharpe et al., 2007). Gerber (1999) subdivided the Lower Sediments into different layers (Fig. 2.2). He described the York Till as a 1-m thick boulder deposit that is the oldest preserved Quaternary unit of Pre-Wisconsinan age (approximately 135,000 years BP) (Kassenaar and Wexler, 2006). The Don Formation consists of sandy storm deposits and peaty muds (Eyles and Clark, 1988). These units are thin and may be missing in many stratigraphic sections. The Scarborough Formation which indicates the onset of the Wisconsinan glaciation overlies the Don

Formation and is composed of clay- to sand-size sediment deposited as a delta around 60,000 years ago (Eyles and Eyles 2002; Sharpe et al., 2018). This layer can reach up to 50 m in thickness and provides a source of water to deep municipal wells. The Sunnybrook Diamict overlies the Scarborough Formation, and is comprised of interbedded sand, diamict, and laminated clay. The Sunnybrook is overlain by the Thorncliffe Formation, which includes glaciolacustrine sand, silt and clay. The Thorncliffe Formation forms the Middle Aquifer that was deposited between 30,000 to 50,000 years ago. The Thorncliffe Formation is separated from overlying aquifers in the ORM by the Newmarket Till (Eyles and Eyles, 2002).

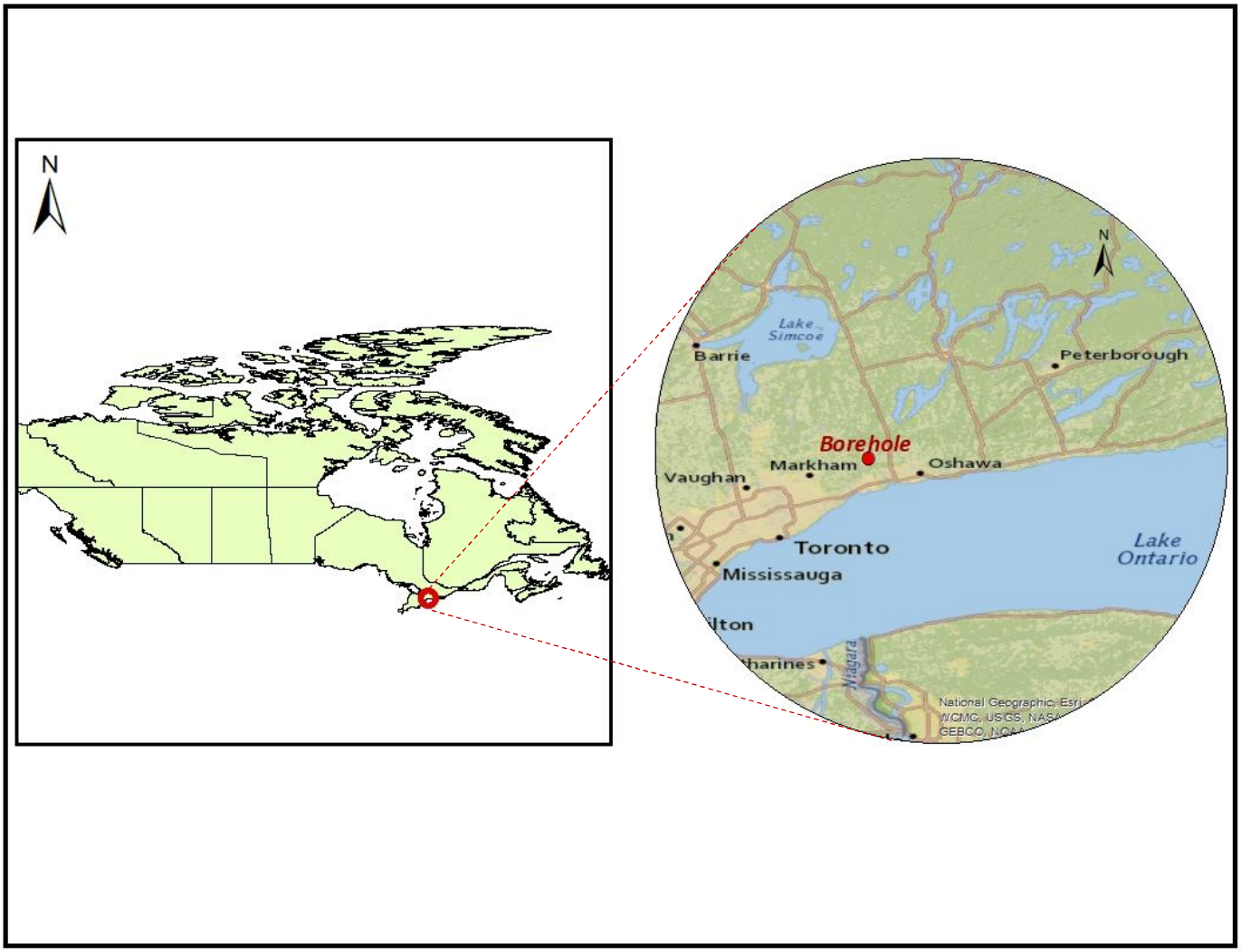

Fig. 2.1. The geographic location of the Pickering borehole, Ontario, Canada

During the Late Wisconsinan, the Newmarket Till (also referred to as the Northern Till) was deposited by the Laurentide ice sheet. It is a regionally extensive confining unit and separates the upper aquifer systems associated with the ORM sediments from the lower aquifer systems that occur within deposits of the Scarborough and Thorncliffe formations (Wexler et al., 2004 ; Kassenaar and Wexler 2006). It is dense, stony (5 – 15% gravel), sandy (38%) silty (~47%) diamicton that ranges from 1 to 69 m thick (Logan et al., 2001). The mineral assemblage contains K-feldspar, quartz, calcite, dolomite, plagioclase, clinopyroxene, and amphibole; these grains range in size from ~2 to 1000 μm (Kjarsgaard et al., 2018). The advance of the Late Wisconsinan ice sheet from the north and along the Lake Ontario basin led to initial deposition of the Newmarket Till into standing water (Sharpe et al., 1999). The Newmarket Till has low porosity, resulting in very low permeability (Gerber, 1999). The Newmarket Till upper surface is commonly drumlinized (Barnett et al., 1998) and the flow of water beneath the ice caused the formation of tunnel channels. The Newmarket Till may allow for 30 to 40 mm of recharge to the Lower Sediments through small-scale structural heterogeneities (Gerber and Howard, 1996). Networks of channels eroded into the till will create regional heterogeneity and influence recharge through the Newmarket Till (Sharpe et al., 2002). The Newmarket Till is characterized by high seismic velocities (2200 m/s to 2800 m/s) in downhole seismic logs acquired over widespread areas and the differences in velocity between Newmarket Till and overlying sediments make it an important reflector on seismic profiles (Sharpe et al., 2018; Kassenaar and Wexler 2006; Boyce, Eyles, and Pugin 1995)

The ORM deposits are usually sands and gravels with local deposits of silt and clay. The ORM can reach up to 150 m in thickness and is tapped by many private wells. Because the ORM sediments are mostly permeable, these wells are sensitive to contamination. The ORM is often used as a stratigraphic marker to distinguish the older Newmarket Till from the younger Halton Till (Gerber and Howard 2000; Sharpe and Russell 2013). Along the southern edge of the ORM, the fine-grained,

silty Halton Till forms the surface unit over much of the southwestern part of the ORM. The Kettleby Till, which has a similar stratigraphy to the Halton Till, covers the north part of the ORM (Sharpe et al., 1996; Logan et al., 2001). The Halton Till is a low permeability unit (Sharpe and Russell, 2013) and it is typically less than 15 m thick but ranges up to 30 m thick (Sharpe et al., 2007). Figure 2.2 shows the simplified diagram of the stratigraphy in the ORM. The thickness of each unit is highly variable and one or all the units can be missing in specific locations.

The Geological Survey of Canada (GSC) in collaboration with Rick Gerber (Oak Ridges Moraine Groundwater Program) developed the stratigraphic log for the Pickering borehole which is summarized in Figure 2.3 Based on the stratigraphic column for this borehole, the sediments are divided into two main groups: the Newmarket Till and the Thorncliffe Formation.

(a)

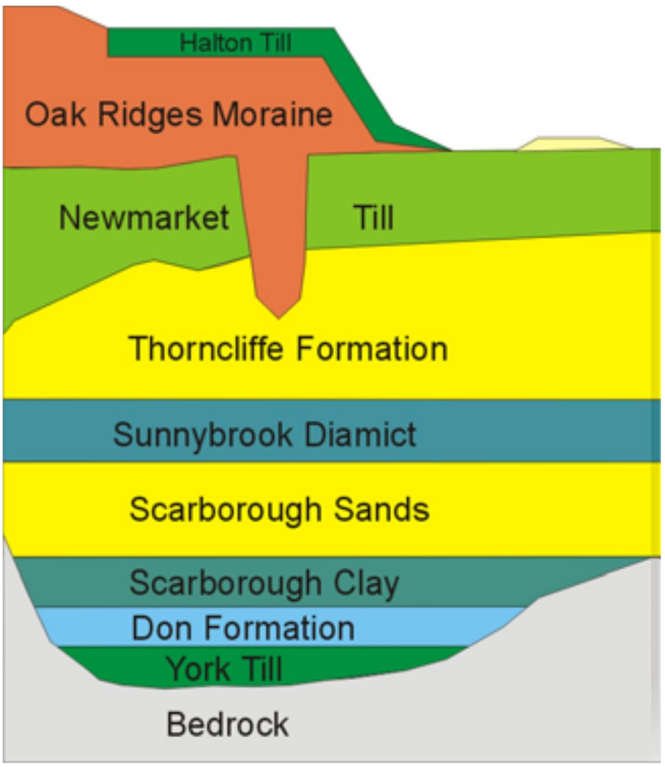

(b)

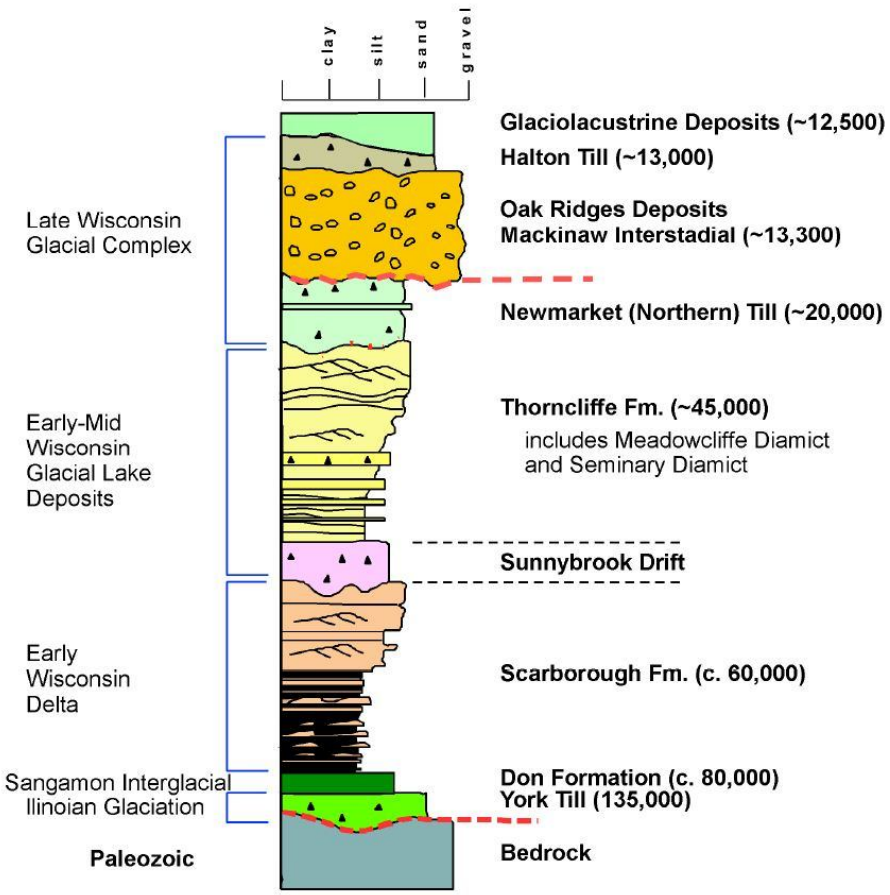

Fig. 2.2. Quaternary sequence. a) The simplified stratigraphy of the ORM and underlying units (Wexler et al., 2004), b) Stratigraphic column (Eyles and Eyles, 2002)

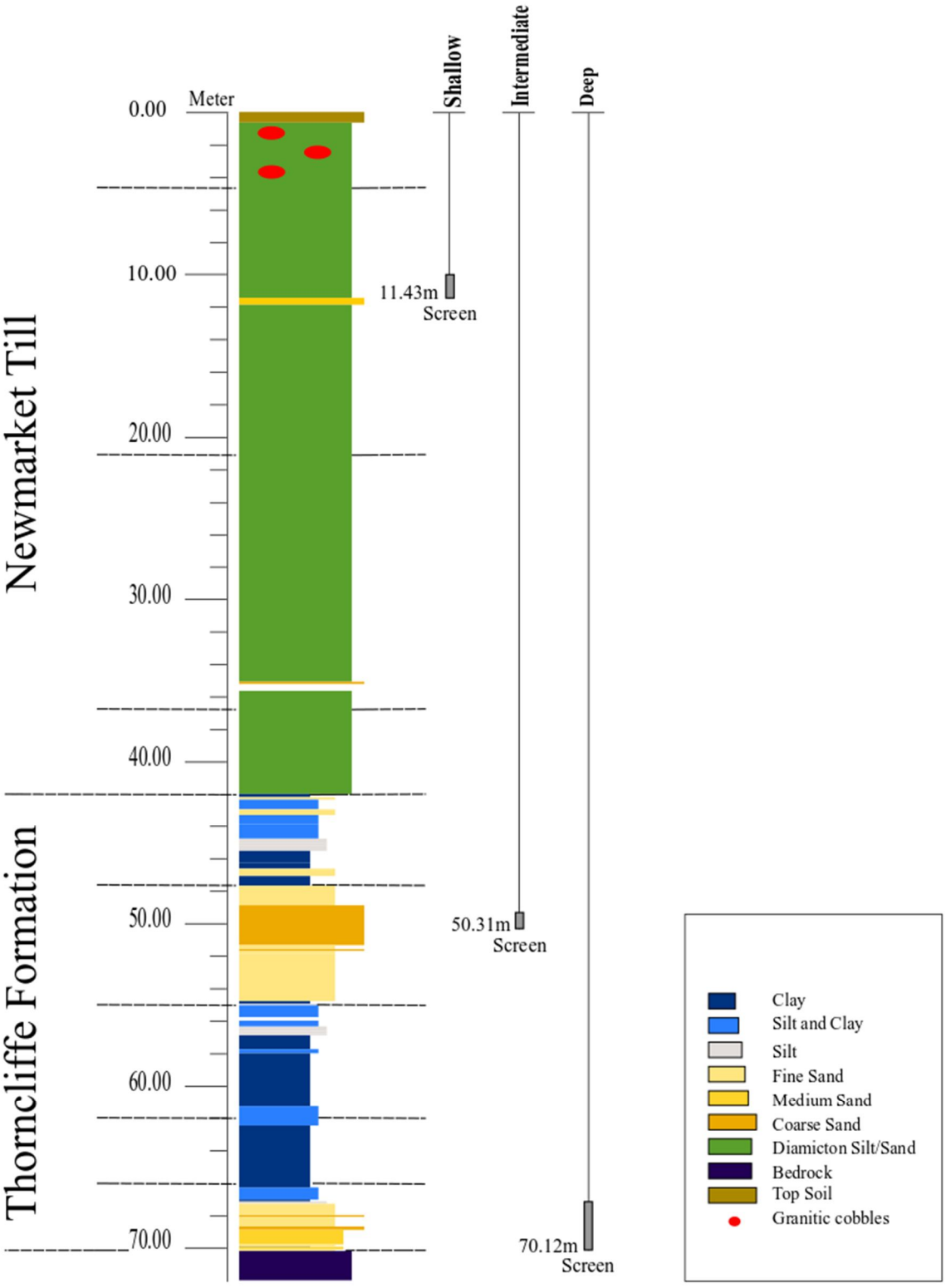

Fig. 2.3. Generalized composite stratigraphic log from the Pickering borehole, modified after (Knight et al., 2019)

2.3. Methods

2.3.1. Sample Collection and Preservation

This study acquired data from the Newmarket Till aquitard and overlying aquifers using piezometers and bored sediment cores. The borehole was completed using PQ wireline drilling techniques in October 2017. Sediment cores were collected in a 85 mm core barrel containing an inner split tube. For groundwater sampling, 3 PVC piezometers were installed in the borehole at the depths to the bottom of the screened interval (11.43 m, 50.31 m, and 70.12 m).

Subsamples of the drill core for porewater analysis were taken in the field. In order to capture detailed inflections in tracer concentrations, the drill-cores were sub-sampled at intervals as small as 0.1 m near boundaries with the surface, internal high-K layers, and the underlying aquifers; however, sampling intervals extended to as much as 3 m within the till. To minimize contamination of porewater by drilling fluids the outer 10 to 20 mm of each core sample was removed with a knife and then discarded. The samples were vacuum sealed in double vacuum sealed plastic bags and stored at 4 ^{o}C prior to analysis.

2.3.2. Measurements and Analysis

2.3.2.1. Porosity

At selected depths, a cylindrical copper tube of known volume was pressed into the core to extract a sub core, also of known volume. The sample was removed and doubly vacuum-sealed in polyethylene bags.

In the lab, the initial wet mass was measured, and then the samples were sequentially dried in the oven (60 °C) until there was no detectable change in their mass. Assuming a water density of 1 kg/m^3, the porosity was calculated by normalizing the water volume in the sample to the total sample volume.

2.3.2.2. Stable Isotopes of water ($\delta^{18}O$ & $\delta^{2}H$)

The vacuum distillation (VD) method involves heating the sample (sediment) under vacuum and water is recovered with an on-line liquid nitrogen trap. In the VD process, the water was extracted and quantified for each sample and converted to volumetric porosity using the densities of the solid and water. Based on the average water content (9.8 %) the appropriate amount of sediment needed to collect 1.5 mL of water was approximately 15 g. The sample was measured into an erlenmeyer flask (25 mL) and installed on the heater side of a vapor-transfer line. A 12 mL Labco exetainer with a septum cap was fitted on the opposite side. The Erlenmeyer flask was submerged in a liquid nitrogen bath to freeze the sample and after about 15 minutes the lines were evacuated to 30 mTorr. The line was disconnected from the vacuum pump and the nitrogen bath was transferred to the bottom of the exetainer. The erlenmeyer flask was placed into an insulated resistance oven and the temperature of the rock samples was slowly increased to 115℃ over a period of 30 minutes. The maximum temperature for heating (115 °C) was determined by experiment to prevent the mixing of $\delta^{18}O$ and $\delta^{2}H$ from mineral sources (some minerals such as gypsum $CaSO_4 \cdot 2H_2O$ will lose their water molecules at high temperature) with the porewater. The water vapour pressure gradient caused porewater to transfer through the line to the cold trap.

To calculate the fractional water yield, the samples were completely dried in the oven for 24 hours at 60 °C to measure the residual water content. The extracted data are considered reliable because fraction of the residual water over the total water mass was less than 5 %.

Samples were analyzed with the Triple Isotope Water Analyzer (TIWA-45EP) by Los Gatos Research (LGR) in the Jan Veizer stable isotope laboratory at the University of Ottawa. The analytical precision of these measurements for $\delta^{2}H$ was 0.5‰ and 0.1‰ for $\delta^{18}O$. The $\delta^{18}O$ of a sample relative to VSMOW (Vienna Standard Mean Ocean Water) is calculated as follows:

$$\delta^{18}O\ (‰) = \left(\frac{\left(\frac{^{18}O}{^{16}O}\right)_{Sample} - \left(\frac{^{18}O}{^{16}O}\right)_{Reference}}{\left(\frac{^{18}O}{^{16}O}\right)_{Reference}} \right) \times 1000 \qquad \text{Eq. 2.1.}$$

2.3.2.3. Nitrate (NO_3^-) and Chloride (Cl^-)

The concentrations of aqueous solutes (Cl^- and NO_3^-) in porewater were determined by leaching the sediments (30 g) with 15 g of MilliQ water for 15 minutes. Phase separation was conducted by centrifugation and filtration (0.45 μm) (Clark et al., 2013, Celejewski et al., 2018). The leachate was then analyzed by ion chromatography (IC).

2.3.2.4. Ammonium (NH_4^+)

Ammonium strongly partitions to cation exchange sites, so extractions targeted the combined NH_4^+ from the porewater and the exchange sites. Using a method modified after that of Bremner and Keeney (1966) and Banwart et al., (1972), 35 g of 2M KCl was used to extract total NH_4^+ in 3.5 g (wet mass) of sediment. The mixture was immersed in an ultrasonic bath for 50 minutes and then phase separation was conducted by centrifugation (4200 rpm, 10 min) followed by filtration (0.45 μm nylon). The NH_4^+ concentrations in the extraction solutions were determined using the salicylate method (Bremner and Keeney, 1966; Baethgen and Alley, 1989; Bower and Holm-Hansen, 1980) with colorimetric measurements conducted with UV-VIS spectrophotometry (650 μm; Ocean Optics USB 4000). The analytical precision was determined from replicate measurements on replicate core samples (RSD = ± 5%).

The extracted mass of NH_4^+ was converted to equivalent porewater concentration (C_{pw}) using the gravimetric water content (w) determined from an adjacent, paired sample by drying at 60 °C.

$$w = \frac{wet\ mass - dry\ mass}{wet\ mass} \qquad \text{Eq. 2.2.}$$

The mass of porewater (M_{pw}) in the extracted sample is:

$$M_{pw} = wet\ mass \times w \quad \text{Eq. 2.3.}$$

The mass of the extraction solution ($M_{solution}$) is the sum of the masses of hypochlorite, salicylate, porewater and 2M KCl.

$$M_{solution} = M_{hypochlorite} + M_{salicylate} + M_{pw} + M_{2M\ KCl} \quad \text{Eq. 2.4.}$$

If the extraction solution has an NH_4^+ concentration of $C_{solution}$ (mg/kg), then C_{pw} (mg/kg; including NH_4^+ in porewater and on ion exchange sites) is:

$$C_{pw} = C_{solution} \times \frac{M_{solution}}{M_{pw}} \quad \text{Eq. 2.5.}$$

2.3.2.5. $\delta^{15}N$ ($N\text{-}NH_4^+$)

Following extraction of NH_4^+ with 2M KCl, subsamples were acidified with sulphuric acid to a pH < 4 and then stored in a freezer (-18 °C) prior to analysis. Analyses of $\delta^{15}N\text{-}NH_4^+$ were conducted at the Environmental Isotope Lab at the University of Waterloo. In a sealed serum vial, NH_4^+ (minimum 1.0 mg L^{-1}) was converted to NH_3 gas by adjusting the pH. The NH_3 is trapped on an acidified quartz glass filter disk enclosed in a gas permeable, hydrophobic membrane (modified PTFE acid trap diffusion method, Brooks et al., 1989). The disk is then analyzed on a Costech 4010 EA-Thermo Instruments Deltaplus XL isotope ratio mass spectrometer (IRMS). The analytical precision was ± 0.5‰. The $\delta^{15}N$ of a sample relative to atmospheric air standard is calculated as follows (Bedard-Haughn et al., 2003):

$$\delta^{15}N\ (‰) = \left(\frac{\left(\frac{^{15}N}{^{14}N}\right)_{Sample} - \left(\frac{^{15}N}{^{14}N}\right)_{Standard}}{\left(\frac{^{15}N}{^{14}N}\right)_{Standard}} \right) \times 1000 \quad \text{Eq. 2.6.}$$

2.3.2.6. Groundwater

Sample bottles were pre-cleaned with de-ionized water in the laboratory and in the field, the bottles were triple rinsed with sample water (pre-filtered as necessary) before the samples were collected. Water samples for dissolved organic carbon (DOC) and DIC were filtered using 0.45 μm filters (nylon) and stored at 4 °C in amber bottles.

Samples for dissolved methane (CH_4) were collected in a Wheaton bottle (1000 mL), acidified with 6N HCl (pH less than 2), and the bottles were sealed with a butyl septum without headspace. In the lab, CH_4 concentrations were measured by creating a headspace by gently displacing the water by high purity helium, typically 10% of the total bottle volume. The bottle is shaken for 5 minutes. The exsolved gases were analyzed by gas chromatography (GC) for N_2, O_2, CH_4, C_2H_6, C_3H_8, C_4H_{10}, and C_5H_{12}(SRI GC 8610C). For hydrogen and carbon isotopes in CH_4, the CH_4 was isolated by GC using a Poraplot Q column on a HP 7890A GC and isotopic measurements were made with a Delta-V Thermo IRMS interfaced to the GC.

The samples were submitted to the Jan Veizer lab at the University of Ottawa to measure the concentration of DIC and DOC and $\delta^{13}C$ isotope ratio in DIC and DOC with the above-mentioned method.

Samples for ^{14}C analysis were collected in Wheaton amber glass bottle using prebaked (500 ˚C for 3 hours) 0.7 μm glass fiber filter (GF/F). Radiocarbon analyses (^{14}C) were performed on a 3MV tandem accelerator mass spectrometer (AMS) built by High Voltage Engineering (HVE) (Crann et al., 2017). The errors on ^{14}C ages (1σ) are based on counting statistics and $^{14}C/^{12}C$ and $^{13}C/^{12}C$ variation between data blocks.

2.3.2.7. $\delta^{13}C$ in Solid Organic Carbon (SOC) and $\delta^{15}N$ in sediment

The sediments contain approximately 40 % calcite (Gerber, 1999) which had to be removed before extracting the organic carbon for $\delta^{13}C$ (SOC) measurements. The calcite was removed by leaching the sample in 10% HCl for 24 hours following the method described by (Midwood and Boutton, 1998). This step was repeated until there was no visible indication of effervescence indicating that calcite had been removed from the sample. The samples were then rinsed with deionized water three times. The residual material was dried at 60 C° for three days. After drying, a known amount of sample was transferred to a tin capsule and tungsten oxide (WO_3) was added as a combustion catalyst. Then, the tin capsules were closed in preparation for elemental analysis.

Elemental analysis is the determination of the elemental composition of organic or inorganic compounds. The Elemental Vario Isotope Cube is to determine %N and %C. The analytical precision (2 σ) for the analyses is ± 0.1%.

In order to measure the $\delta^{13}C$ and $\delta^{15}N$ in solid sediments, the tin capsules were loaded into an elemental analyzer (EA) interfaced with an IRMS. The sample was flash combusted at about 1800 °C (Dumas combustion) and the resulting gas products carried by helium through columns of oxidizing/reducing chemicals optimized for CO_2 and N_2. The gases were separated by a “purge and trap" adsorption column and sent to IRMS.

2.3.2.8. ^{14}C in Sediment

For ^{14}C measurements in sediment, carbonates were removed by acid wash (HCl, 1N, 80°C, 30 min) followed by three rinses in Milli-Q water. Clean samples were freeze-dried overnight. Freeze-dried samples were combusted, graphitized and submitted to the Accelerator Mass Spectrometer (AMS) for analysis (Crann et al., 2017).

2.3.2.9. Diffusion

X-ray radiography is a non-destructive method applied to a constant source in-diffusion experiment to assess diffusion properties of the Newmarket Till. The method used is outlined by Cavé et al., 2009 where changes in attenuation data, $\Delta\mu$, of an x-ray attenuating tracer is captured by a polychromatic cone-beam x-ray source over time as it diffuses through the sample. This method was done for 7 samples by Dominique Bower (2019) in her BSc Honours project. Diffusion experiments were conducted on cylindrical samples (20 mm diameter, 20 mm length) mounted in contact with a tracer solution reservoir while remaining isolated from the atmosphere. Diffusion experiments were conducted using an iodide tracer solution which could diffuse upwards through the samples from the lower reservoir. The tracer solution was made using NaI and $Ca(OH)_2$ and added to a separate 1 kg of deionized water.

2.4. Results

According to Figure 2.4, the sediment porosity varies from 13 to 44% with an average of 25%. More specifically, porosity values remain at about 20% from the top of the stratigraphy column until the depth of 42 m in the bottom of the Newmarket Till. However, below this unit, in the Thorncliffe Formation, the porosity value increases to about 44% at the depth of 69 m. The highest porosity values are observed in the clay and sand part of the Thorncliffe Formation. Figure 2.4 also compares the gravimetric water content values to the volumetric porosity, and they are in good agreement.

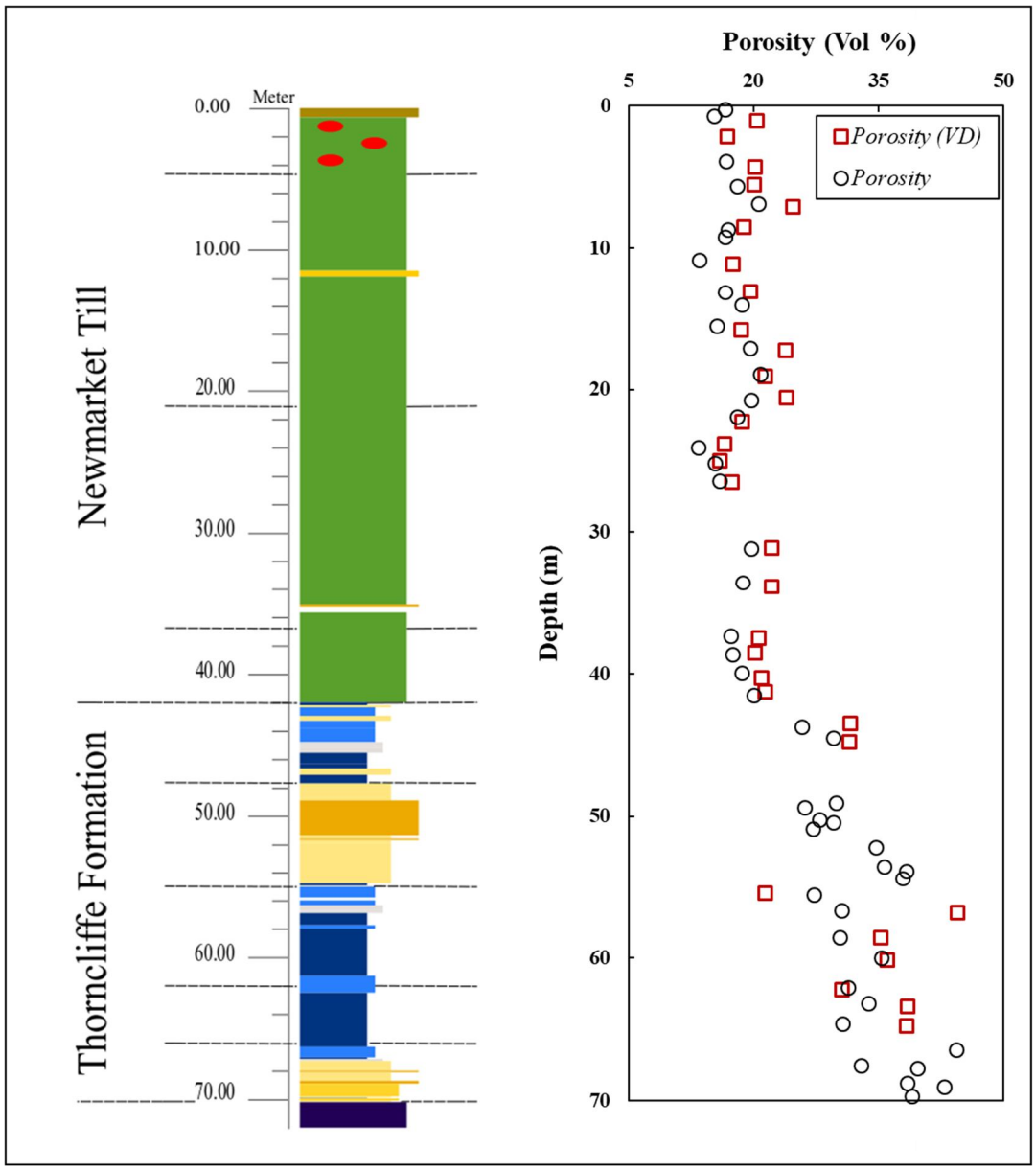

Fig. 2.4. Comparison of volumetric porosity from direct measurements (circles) vs. values calculated from extracted water mass and mineral grain densities (squares).

The results of oxygen and hydrogen isotope analyses in groundwater and porewater are presented on Figure 2.5. The δ^2H values of 31 porewater samples range from -112 to -67 ‰ while $\delta^{18}O$ values range from -16 to -9.6 ‰ VSMOW. Furthermore, for both $\delta^{18}O$ and δ^2H, values are higher near the surface, ranging from -11 to -9.6 ‰ and -75 to -67‰, respectively, down to the depth of 25 m. In the deeper part of the Thorncliffe Formation, a decreasing trend can be seen for both isotopes (to as low

as -16 ‰ for $\delta^{18}O$ and -112 ‰ for $\delta^{2}H$). In addition, the groundwater results for the piezometers indicate that the $\delta^{18}O$ and $\delta^{2}H$ have ranges from -11.7 to -11 ‰ and -78.2 to -73.6 ‰, respectively. In Figure 2. 6, values of $\delta^{18}O$ are plotted versus $\delta^{2}H$ for all porewater, groundwater and local meteoric water samples (Egbert, ON; Fig. 2.7). The best-fit regression for porewater samples is $\delta^{2}H = 7.22\ \delta^{18}O + 2.15$ with a correlation coefficient of $r^2 = 0.95$ (Fig. 2.6).

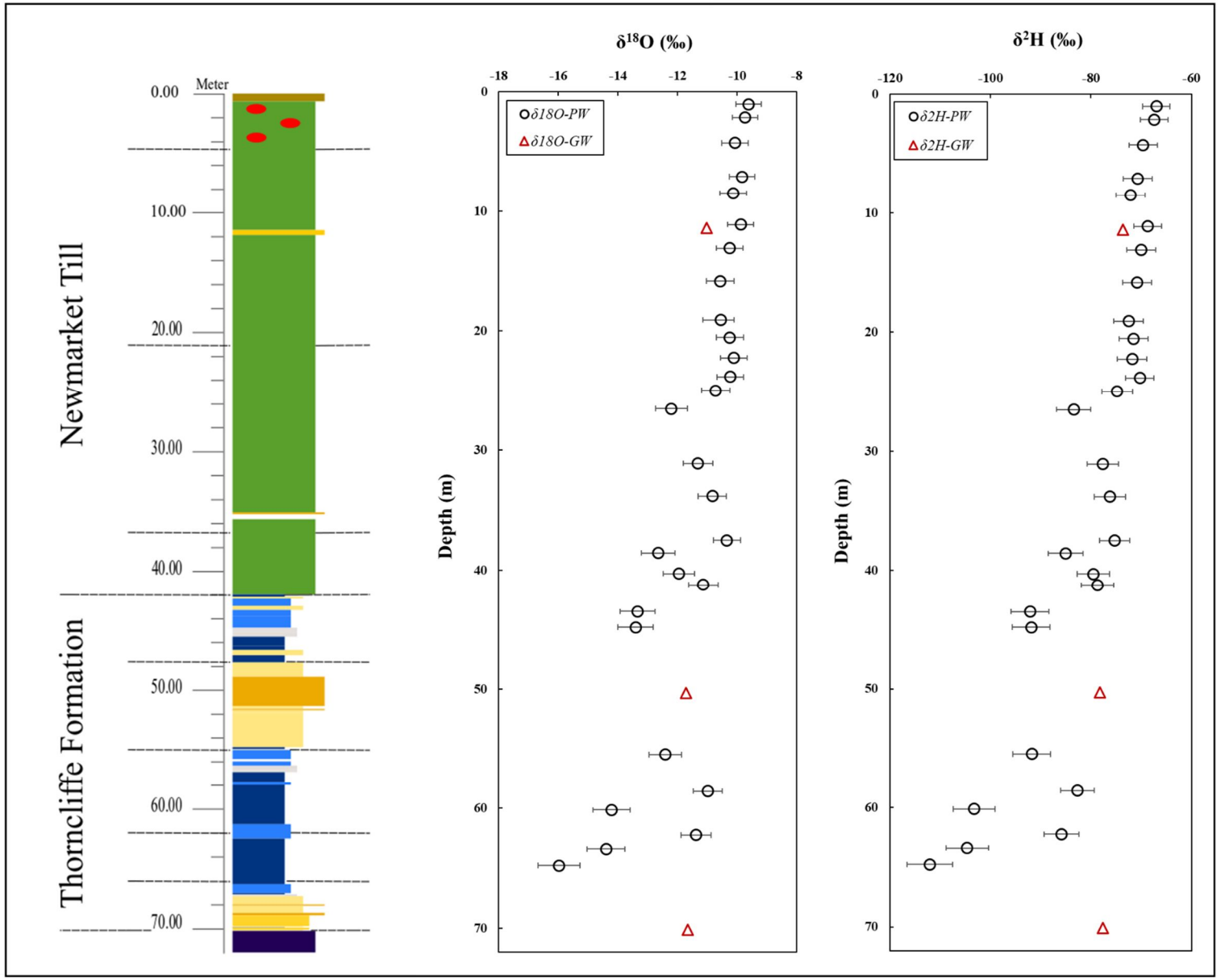

25

Fig. 2.5. Vertical profile distribution of $\delta^{2}H$ and $\delta^{18}O$ versus depth. Error bars indicate one standard deviation (SD)

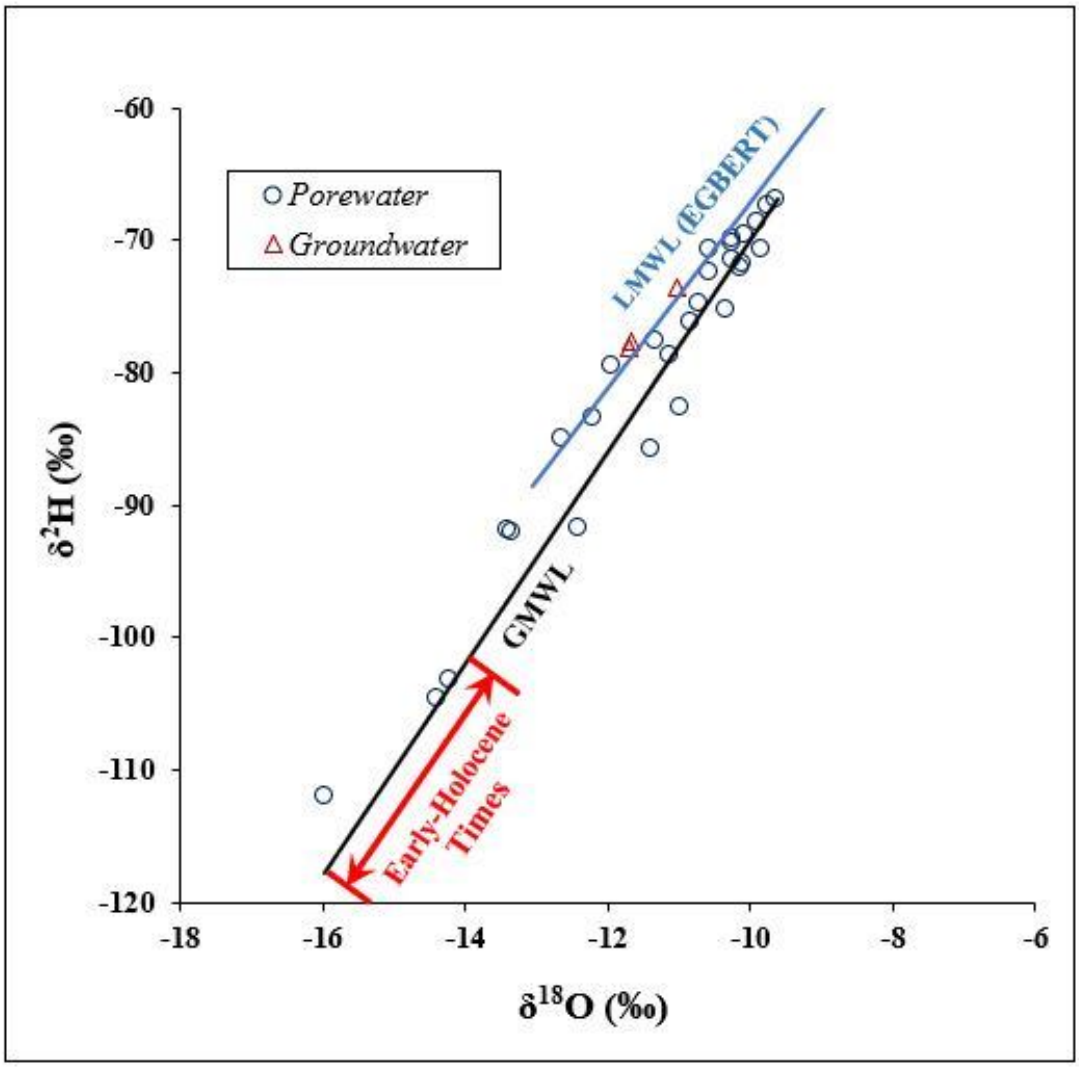

Fig. 2.6. δ^2H vs. $\delta^{18}O$ values of the porewater samples and groundwater samples. Global Meteoric Water Line (GMWL), Local Meteoric Water Line for Egbert (LMWL), and the range of δ^2H vs. $\delta^{18}O$ for early-Holocene times (Edwards et al., 1996)

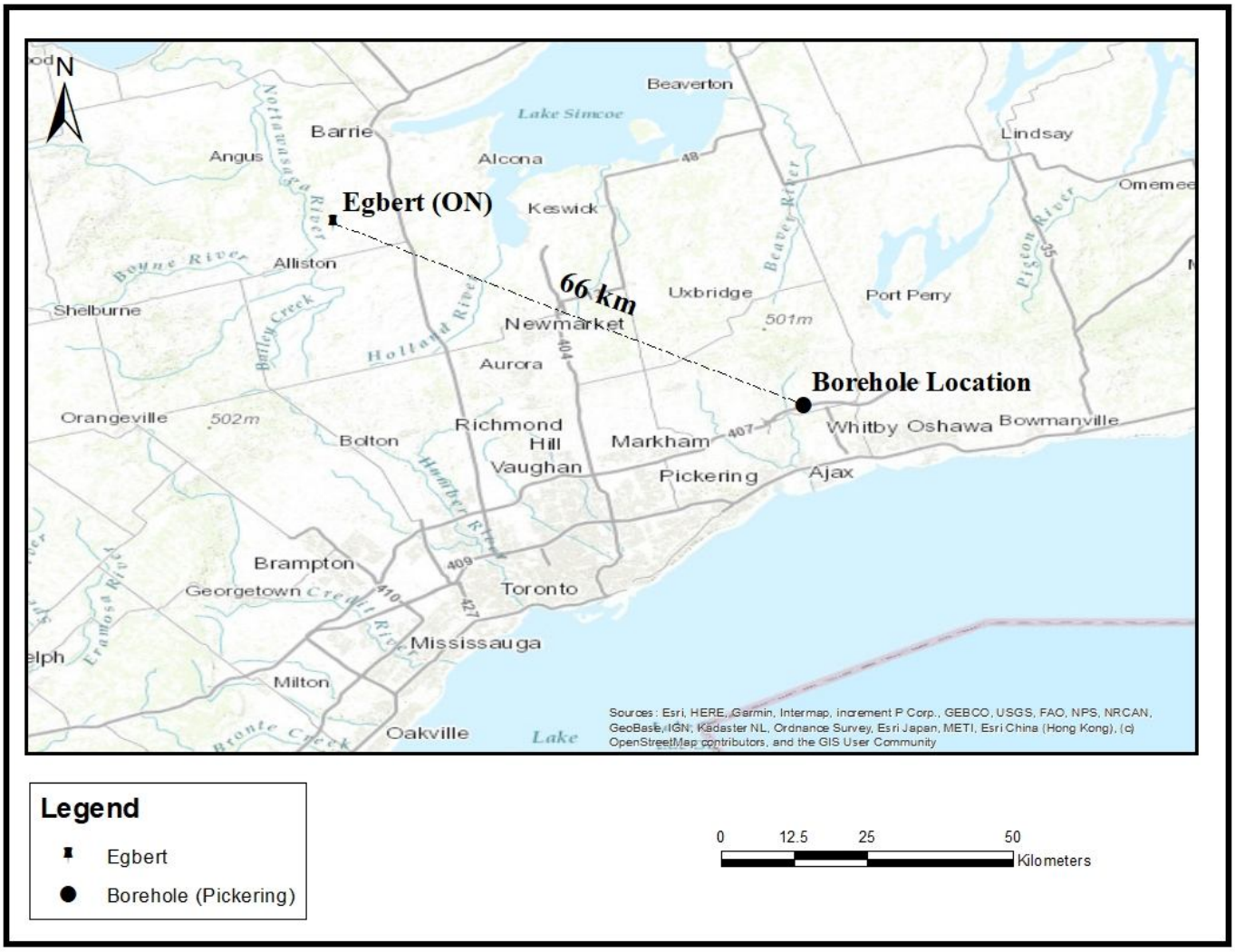

Fig. 2.7. Location of borehole and distance from Egbert, ON

Nitrate (NO_3^-) and chloride (Cl^-) concentrations were measured in the 31 samples and range from 0.03 to 34.25 ppm and 3.93 to 39.06 ppm, respectively (Fig. 2.8). The vertical profile of NO_3^- concentrations indicates that the maximum value occurs near the surface at the depth of 2 m, and low concentrations (< 2 ppm) are consistently observed in the remaining depths. Approximately 94% of the samples have NO_3^- concentrations below the WHO limit for drinking water (10 ppm). A similar trend can be observed for Cl^- concentration; the highest Cl^- concentration (39.06 ppm) occurs at the depth of 4 m and concentrations are less than 13 ppm in the rest of the Newmarket till and Thorncliffe Formation.

Total extractable NH_4^+ concentrations vary from 4.09 to 515 ppm with an average value of 137.42 ppm. According to Figure 2.9, the total extractable NH_4^+ concentration is low near the surface (4 to 6 ppm). The NH_4^+concentration increases gradually to approximately 60 ppm at a depth of 11 m and then remains nearly constant from 11 to 45 m, which is the bottom of the Newmarket Till. Near the top of the Thorncliffe Formation, extractable NH_4^+ concentrations increase to 170 ppm and below the middle aquifer where the Thorncliffe Formation are comprised of fine-grained, relatively organic-rich clayey muds NH_4^+ concentrations increase gradually to the maximum of 515 ppm.

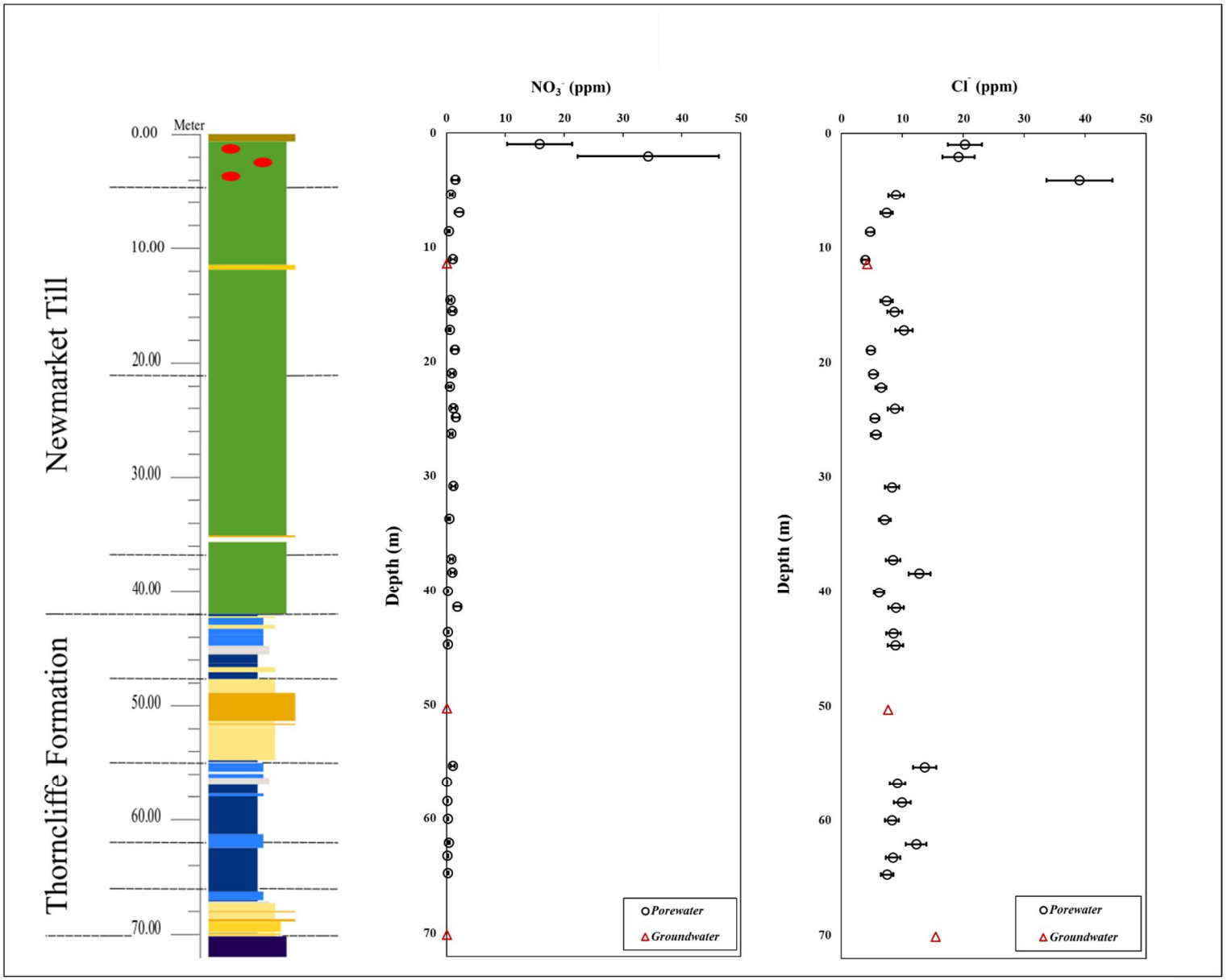

Fig. 2.8. Vertical distribution of NO_3^- and Cl^- versus depth. Error bars indicate one standard deviation (SD)

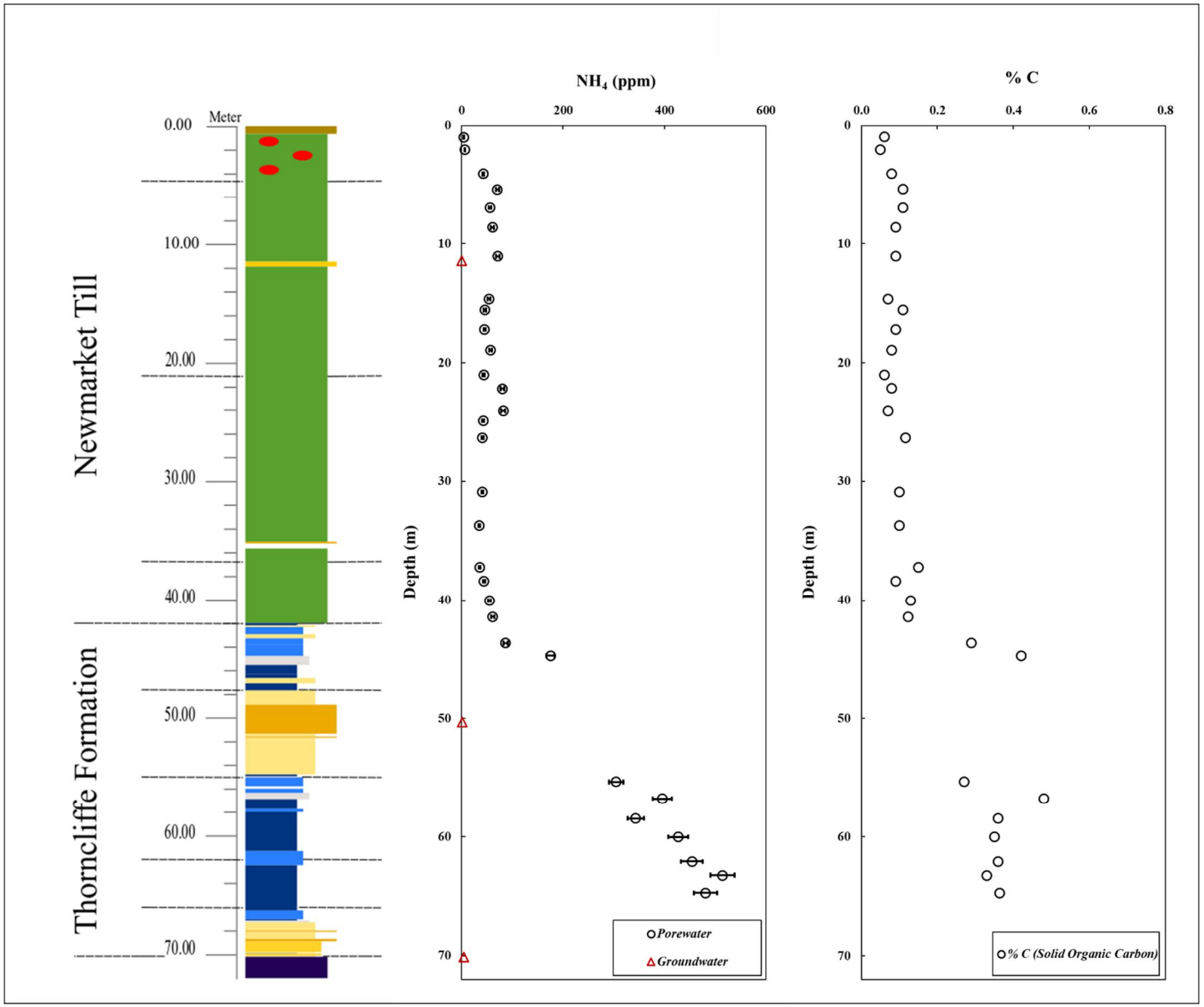

Fig. 2.9. Vertical distribution of NH_4^+ (that the porewater values are total extractable NH_4^+ while the groundwater values are aqueous NH_4^+ concentrations) and solid organic carbon content vs. depth. Error bars indicate one standard deviation (SD)

Figure 2.10 displays the $\delta^{15}N$ values that were measured in the extractable NH_4^+ and in the sediments. A limited number of samples (n = 8) of the extractable NH_4^+ were analyzed for $\delta^{15}N$ to evaluate sources of N. The $\delta^{15}N$ values for the extractable NH_4^+ range from -1.40 to 8.01‰ with an average value of 4.75‰. At a depth of 15 m, the $\delta^{15}N$ value is 0.75‰, decreasing to -1.40‰ at 26 m depth and at the bottom of the Newmarket Till the value increases to 3.7‰. Deeper in the Thorncliffe Formation, the $\delta^{15}N$ values increase to about 8‰ at the depth of 62 m. The $\delta^{15}N$ values for SOC in sediment samples show a very narrow range from 3.8 to 4.9‰ with an average value of 4.3‰.

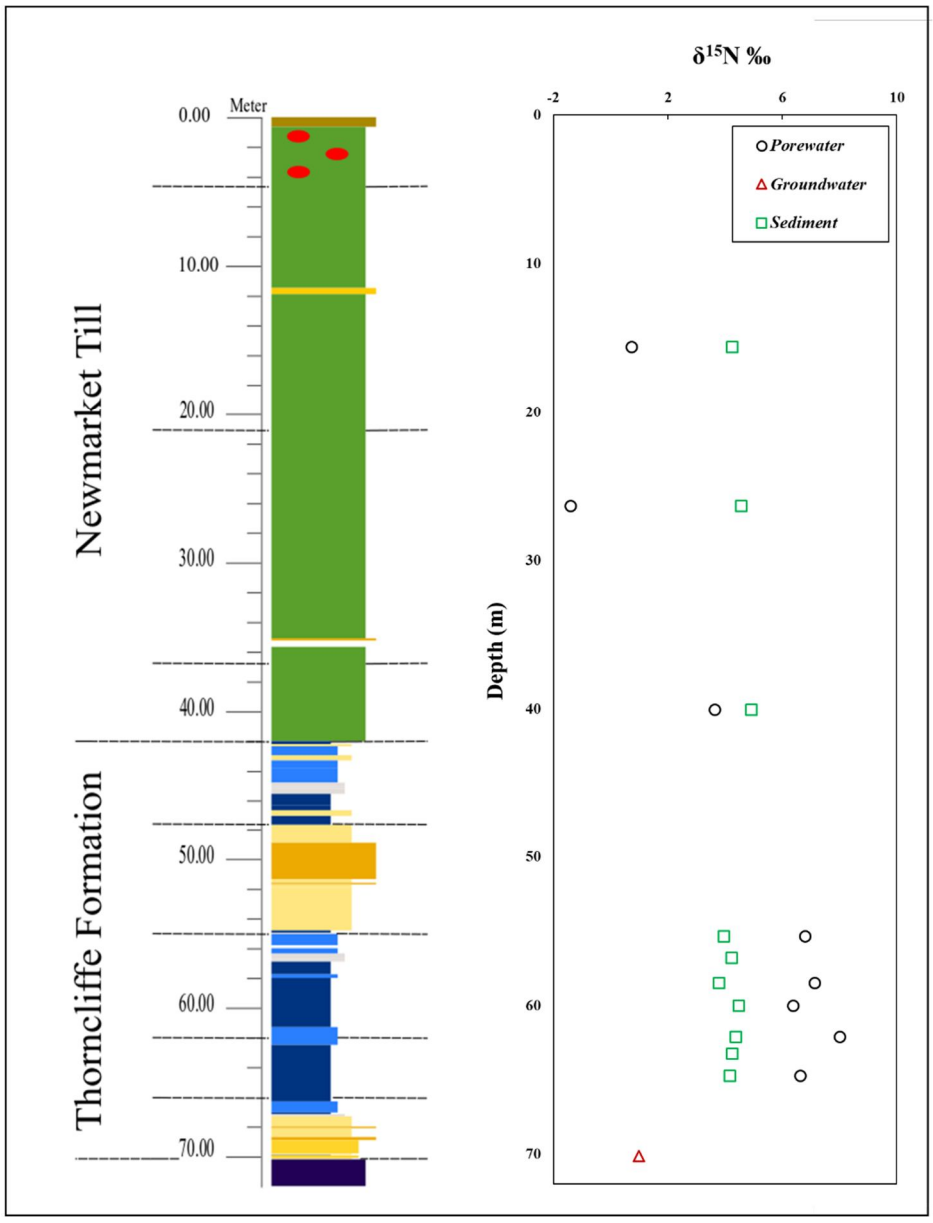

Fig. 2.10. Vertical distribution of $\delta^{15}N$ from extractable aqueous NH_4^+ and solid organic carbon in the sediment vs. depth

The DIC, DOC, and CH_4 analyses for groundwater from the piezometers are presented on Figure 2.11. DIC concentration increases with depth from 37.7, through 56.8, and to 72.9 ppm in the shallow, intermediate, and deep piezometers, respectively. Similarly, DOC concentrations increase with depth from 1.15 to 3.96 and 4.60 ppm, respectively for the shallow, intermediate, and deep piezometers. Methane concentrations follow the same pattern for the shallow, intermediate, and deep piezometers, increasing from 0.07 to 4.51 and 10.5 ppm respectively.

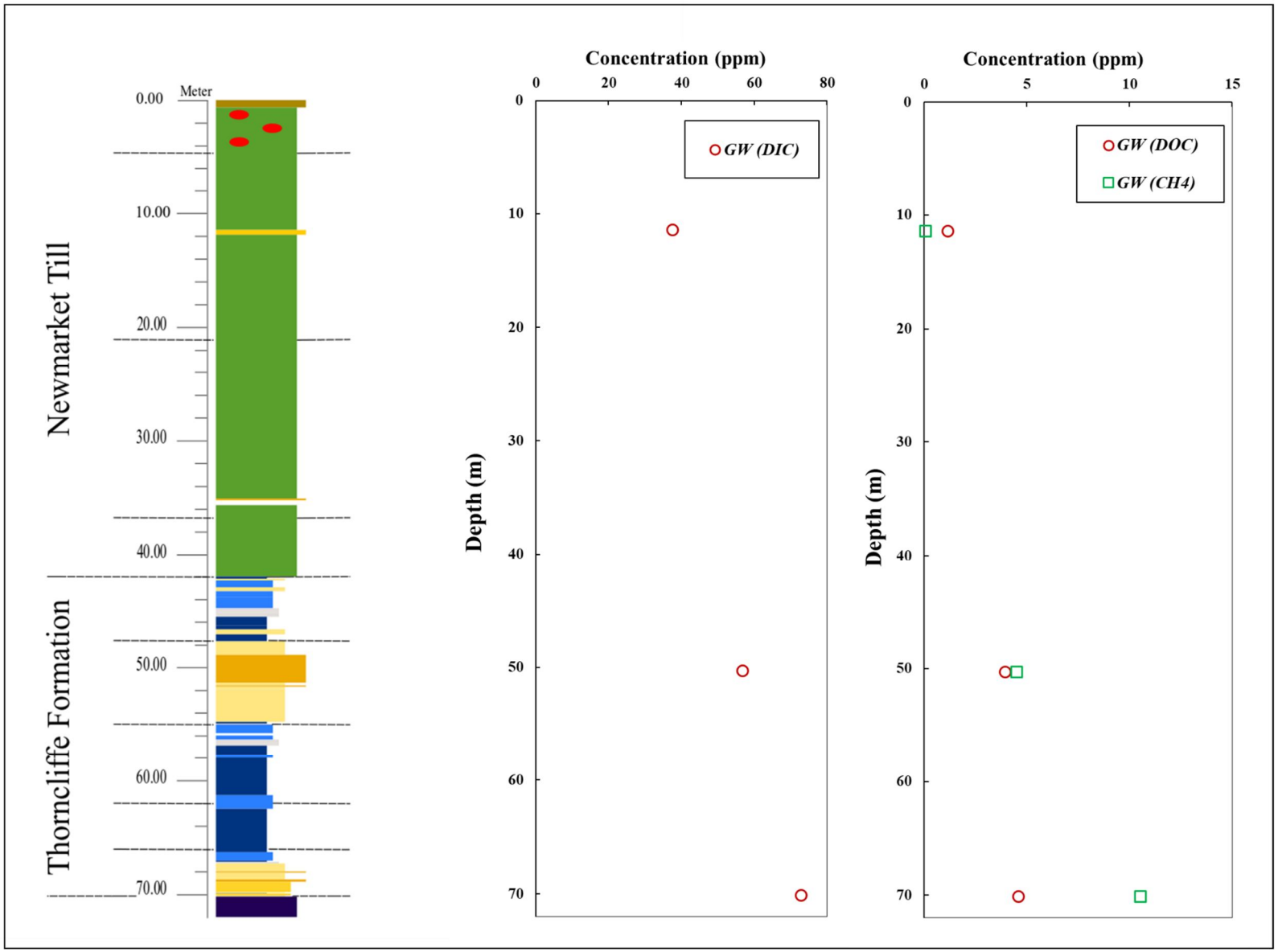

Fig. 2.11. Vertical distribution of dissolved inorganic carbon (DIC), dissolved organic carbon (DOC), and methane (CH_4) concentrations.

The $\delta^{13}C$ value of DIC displays an enrichment trend versus depth in the groundwater increasing from -11.16 ‰ at 11 m depth in the Newmarket Till, to approximately 0.71 ‰ at 70 m at bottom of the Thorncliffe Formation. On the other hand, the $\delta^{13}C$ values for DOC display a slight depletion trend versus depth with values decreasing from -28 ‰ at 11 m to -34 ‰ at 70 m depth (Fig. 2.12). The $\delta^{13}C$ values for SOC are mostly consistent with depth, ranging between -25 ‰ and -30 ‰. The $\delta^{13}C_{CH_4}$ follows a similar trend to the $\delta^{13}C$ in the DOC (Fig. 2.12).

The $\delta^{13}C$ and $\delta^{2}H$ isotope compositions of CH_4 were determined for groundwater from the intermediate piezometer ($\delta^{13}C$ = -83 ‰ and $\delta^{2}H$ = -279 ‰) and the deep piezometer ($\delta^{13}C$ = -77 ‰ and $\delta^{2}H$ = -272 ‰). Whiticar (1999) assigned a wide range of C and H isotope ratios for biogenic CH_4, $\delta^{13}C_{CH_4}$ from -110 to -50 ‰, and $\delta^{2}H_{CH_4}$ from -400 to -150 ‰, all consistent with the isotopic compositions for CH_4 from the intermediate and deep piezometers.

For the ^{14}C, the withdrawn groundwater sample from the deep piezometer has a value of 12.6 % pMC (percent of modern carbon). The ^{14}C value in the sediments have the average value of 0.4 % pMC.

The pore diffusion coefficients (D_p) measured at depths of 5.43 and 42.7 m are $1.87\times10^{-10} \pm 1.99\times10^{-10}$ and $1.98\times10^{-10} \pm 7.86\times10^{-11}$ respectively. The D_p value accounts for the tortuosity of the pore space:

$$D_p = D_0 \cdot \tau_f \qquad \text{Eq. 2.7.}$$

where, D_0 is the free-water diffusion coefficient and τ_f is the tortuosity factor. The D_0 value for Cl^- at 25 °C is 2.03×10^{-9} m^2/s (Yuan-Hui and Gregory, 1974) suggesting that the τ_f values are on the order of 10^{-1}. The effective diffusion coefficient (D_e) accounts for the effect of porosity on the diffusion mass flux:

$$D_e = D_p \cdot \emptyset_w \qquad \text{Eq. 2.8.}$$

where ϕ_w is the fractional water accessible porosity. Given the average porosity of 0.2 (20 %) in the Newmarket till, the measurements indicate an average D_e value of 3.9×10^{-11} m^2/s.

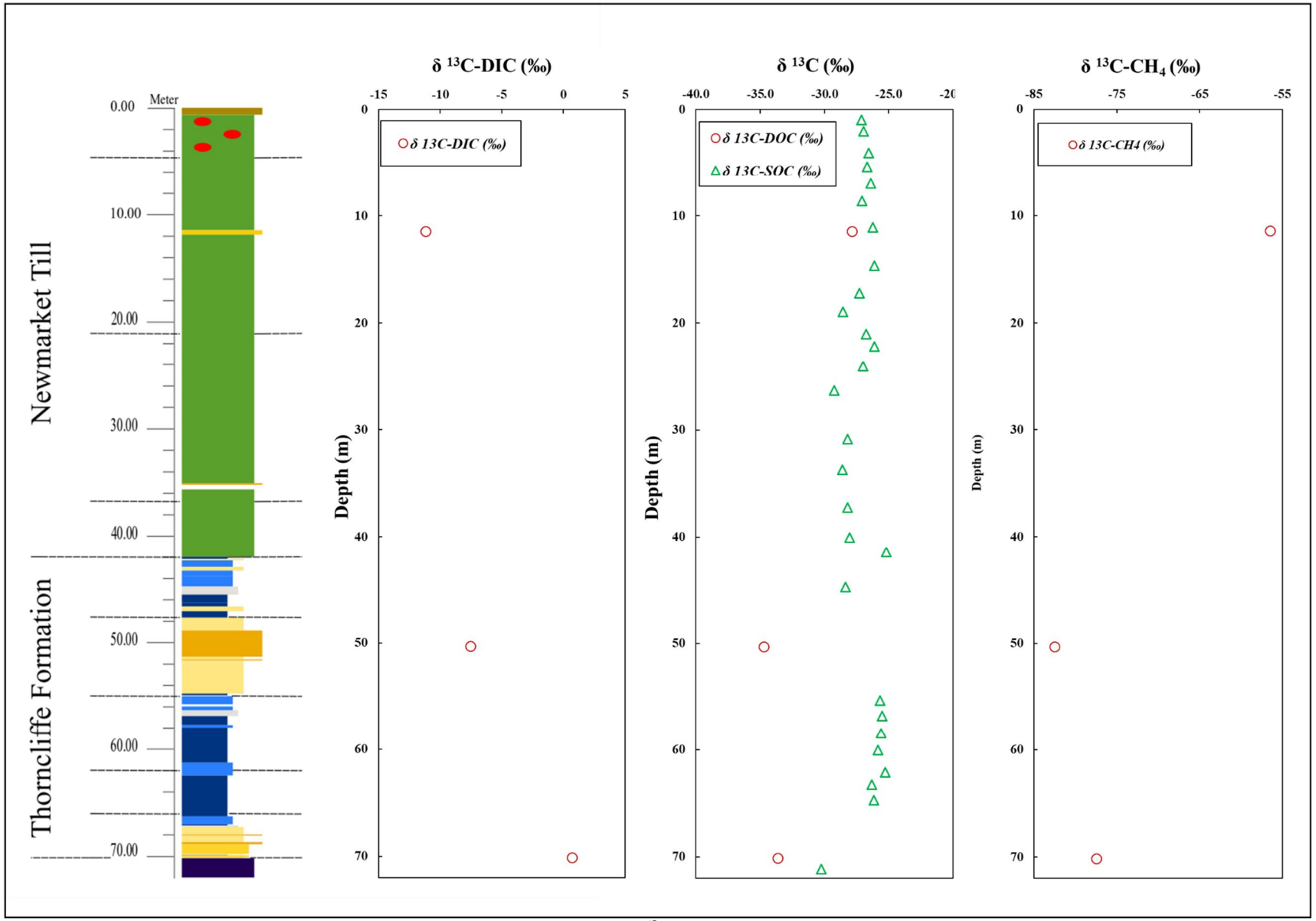

Fig. 2.12. Vertical distribution of $\delta^{13}C$ in DIC, DOC, SOC, and CH_4

2.5. Discussion

The $\delta^{18}O$ and $\delta^{2}H$ values for porewater are commonly used as natural tracers for water of different origin, allowing for an understanding of the rate of solute transport in hydrogeologic systems because they are not significantly affected by mineral-water reactions (Desaulniers et al., 1981; Desaulniers and Cherry, 1989; Gerber and Howard, 1996; Koehler et al., 2000). Figure 2.6 shows the $\delta^{18}O$ versus $\delta^{2}H$ isotopic composition for the nearest Local Meteoric Water Line (LMWL) from Egbert, Ontario (IAEA.database, 2019). The $\delta^{18}O$ and $\delta^{2}H$ values in the annual precipitation in Egbert range from -7 to -13 ‰ and -50 to -90 ‰, respectively. Three groundwater samples and 90 % of porewater samples overlap closely with the LMWL data which suggests that these samples also contain present-day meteoric water.

The history of $\delta^{18}O$ and $\delta^{2}H$ in precipitation for southern Ontario in the late-glacial and early-Holocene times is characterized by relatively depleted values because of cold climate conditions (Hendry and Wassenaar, 1999). The average $\delta^{18}O$ value for the early-Holocene (12,000 yr BP) is around -16 ‰ as reported by Edwards et al. (1996). The stable isotope profiles show a slight depletion trend downward through the Newmarket till, possibly retaining slightly depleted signatures near the bottom that reflect residual early Holocene waters that are almost completely displaced by recent meteoric water. There are three porewater samples with $\delta^{18}O$ values in the range of -14 to -16 ‰ and they are located in the clay-rich portion of the Thorncliffe Formation at depths of 60, 62, and 65 m. These relatively depleted isotope signatures at depth suggest that water in the lower part of the system retains a cold-climate signature, thereby indicating a diffusion-dominated system with long porewater residence time. In contrast, the isotope compositions in the confined aquifers are similar to modern precipitation indicating rapid recharge relative to the slow displacement of early Holocene water from the fine-grained, lower-permeability units. This interpreattion is inconsistent with the results of ^{14}C

analyses of DIC from the deepest confined aquifer (70 m); there the fraction of ^{14}C is 12.6 pMC, which according to Equation 2.9, represents a groundwater age of approximately 16,000 yr B.P if we ignore q which is the correction factor used to account for radiocarbon dilution from dissolution of marine carbonate (calcite) along the flow path from the up-gradient recharge area (Smith et al., 1976; Clark, 2015).

$$t = -8033 \ln\left(\frac{a^{14}C}{q.\ a_0{}^{14}C}\right) \qquad \text{Eq. 2.9.}$$

In Equation 2.9, $a^{14}C$ is the activity of ^{14}C in groundwater DIC, $a_0{}^{14}C$ is the activity of ^{14}C during recharge (assumed to be 100 pMC). When carbonate dissolution takes place the $a_0{}^{14}C$ will be closer to 50 pMC because of dilution with ^{14}C-free carbonate (Eq. 2.10) (Clark, 2015). Therefore, in Equation 2.9, if we consider q = 0.5 the radiocarbon age would be 11000 yr B.P. This radiocarbon age is possible, despite the apparently modern H and O stable isotope composition of the water, because the aquifer is confined by pre-Wisconsinan organic-rich sediments that could provide a diffusion-driven source for old carbon to the aquifer along the recharge path from the surface.

$$^{14}CO_2 + H_2O + CaCO_3 \longrightarrow Ca^{2+} + H^{14}CO_3^- + HCO_3^- \qquad \text{Eq. 2.10.}$$

The elevated concentration of Cl^-, a conservative tracer, near the surface of the depth profile is possibly the result of the agricultural activity, with perhaps a contribution from road salt. The borehole is located in close proximity to Highway 407 (300m; Fig.2.7), but the highway was recently constructed (2015) so agriculture is a more likely explanation than road salt. The large Cl^- concentration gradient near the surface (Fig. 2.8), suggest that the Newmarket till prevents penetration of Cl^- contamination to depth. This is supported by the low D_e value (3.9×10^{-11} m^2/s) that we measured with the non-destructive constant source in-diffusion radiography method.

Nitrate (NO_3^-) shows a similar trend to Cl^- where the concentration of NO_3^- near the surface is much higher than at depth which supports our conceptual model that agricultural fertilizers represent the source for these solutes at the surface. Generally, microbial denitrification renders NO_3^- a non-conservative tracer, although Figure 2.9 indicates that the concentrations of organic C in the Newmarket Till are low, which suggests that the higher concentrations of NO_3^- near the surface and low concentrations at depth are related to low permeability, not denitrification.

Ammonium levels in unpolluted groundwater are generally below 0.2 ppm, but it can be higher in cultivated areas such as farmland. In an uncontaminated reducing environment, NH_4^+ commonly originates from ammonification of organic forms of N via microbial pathways during the decomposition of organic matter (Wang et al., 2013). Similarly, high levels of NH_4^+ in the Thorncliffe Formation are interpreted to result from the ammonification. Elevated concentrations of NH_4^+ in groundwater originating from natural sources have been reported all over the world. For example, in east-central Illinois, USA, elevated NH_4^+ concentrations derived from buried organic material in Robein silt were observed by (Roy et al., 2003). In the Wood River Wetland, Upper Klamath River Basin, USA, Carpenter et al. (2009) reported elevated NH_4^+ that had been released into a confined aquifer from the overlying peat soil. Jiao et al. (2010) observed concentrations of NH_4^+ as high as 390 mg L^{-1} in the basal sand Pleistocene aquifer of the Pearl River Delta, China, that is related to the decomposition of organic matter under reducing condition.

Generally, mineralization of organic N does not generate a significant isotope fractionation (Kendall and Aravena, 2000; Du et al., 2017), which means that the N isotopic compositions of extractable NH_4^+ would be similar to those of the source organic material in the sediments. However, Figure 2.10 indicates that fractionation does occur in this system, with three possible explanations. First, at constant temperature, lighter isotopes will diffuse more rapidly than heavier isotopes (O'leary

et al., 1992; Chanton and Whiting, 1996). In the fine-grained, organic-rich units of the Thorncliffe Formation, between the intermediate and deep aquifers, $^{14}NH_4^+$ will diffuse faster than $^{15}NH_4^+$, migrating preferentially to the bounding aquifers where it is removed from the system. This loss of ^{14}N contributes to the observed enrichment of $\delta^{15}N$. Similarly, the elevated concentrations of NH_4^+ in the Thorncliffe Formation would drive upward diffusion into the Newmarket Till, and faster transport of $^{14}NH_4^+$ relative to $^{15}NH_4^+$ could contribute to the slight depletion of $\delta^{15}N$ in the porewater compared to the solid organic source. Second, the tendency for heavier isotopes to partition more strongly to ion exchange sites (Criss, 1999; Roe et al., 2003; Hoefs, 2009) than light isotopes will enhance the diffusion-related fraction effect by further slowing the transport of the heavy isotopes. Finally, enrichment of $\delta^{15}N$ in porewater of the Thorncliffe Formation could result from dissociation of NH_4^+ to NH_3 under anaerobic conditions:

$$NH_4^+ (aq) \longleftrightarrow NH_3 (aq) \longleftrightarrow NH_3 (g) \qquad \text{Eq. 2.11.}$$

Li et al. (2012) found that at pH above 6, isotopic fractionation can take place during the conversion of NH_4^+ (aq) to NH_3 (aq), and that the NH_3 can degas. The pH values measured from groundwater in the three confined aquifers (Fig. 2.3) range from 7.35 to 8.25, conditions that could support this mechanism of isotopic fractionation.

Most natural materials have negative values for $\delta^{13}C$ which reflect low ^{13}C levels compared to the common standard, Pee Dee Belemnite (PDB) (O'Leary, 1988). Figure 2.12 shows that the values of $\delta^{13}C$-DIC increase with depth. Near the surface, $\delta^{13}C$-DIC has a value of -11 ‰, but it increases with depth to a value of 0.7 ‰. There are two possible explanations for the increasing trend of $\delta^{13}C$ with depth. First, it may be the result of calcite dissolution. Thus, dissolution of carbonate can dilute $\delta^{13}C$ and increase its value. Second, elevated values of $\delta^{13}C$ can result from methanogenesis, so the correlation between increased $\delta^{13}C$-DIC and elevated concentrations of CH_4 in the intermediate and

deep aquifers (50 and 70 m depth) provides confirmation that the CH_4 is biogenic. Archaeal reaction can produce CH_4 by reduction of CO_2 in anaerobic environments (Whiticar, 1999). Under strong reducing conditions, organic matter is used to reduce CO_2 and produce CH_4. During this conversion, the $\delta^{13}C$ will be enriched in CO_2 and it may result in depletion of $\delta^{13}C$-DOC as is observed in Figure 2.12.

2.6. Conclusion

The combined evaluation of multiple datasets provides evidence that the Newmarket Till is an aquitard that effectively protects groundwater in the underlying aquifers. Key evidence includes the occurrence of what appears to be cold-climate water at depth in the system, low diffusion coefficients and lack of evidence for downward transport of NO_3^- and Cl^-, despite the downward hydraulic gradient.

In the Thorncliffe Formation, high levels of NH_4^+ occurred in a reducing environment and showed an increasing trend with depth. High levels of organic C in this part of the system, suggests that the main natural process of generating NH_4^+ should be the mineralization of organic N (ammonification).

Generally, mineralization of N should not generate isotopic fractionation, but in the system, there is fractionation. There are three possible processes that can describe the fractionation: (1) lighter isotopes diffuse faster than heavier isotope, so the rate of diffusion can cause fractionation; (2) heavier isotopes prefer to go to the exchange site and it cause separation along the pathway; (3) dissociation of NH_4^+ to NH_3 under anaerobic condition.

Methane in groundwater is derived from two main sources: biogenic and thermogenic. Biogenic CH_4 was formed during the methanogenesis. The source of CH_4 in the system is biogenic based on using the combination of the stable isotope values of CH_4 ($\delta^{13}C_{CH4}$ and δD_{CH4}). The methanogenesis reactions in the Thorncliffe Formation can be a reason for high values of $\delta^{13}C_{DIC}$. Another reason can be the equilibration of $\delta^{13}C$ with calcite dissolution and dilute the negative $\delta^{13}C$ values.

2.7. Acknowledgements

This investigations were funded by Geological Survey of Canada (GSC). Also, this study was supported by Durham Region and TRCA, Toronto and Region Conservation Authority, as part of the Carruthers Creek watershed plan update study. We have greatly benefited from intensive scientific discussions with Rick Gerber (Oak Ridges Moraine Groundwater Program) and Bruce Kjarsgaard and Hazen Russell (GSC). The authors thank Hamed Mozafari and Magda Celejewski for their assistance in the field work, and Soroush Shahryari Fard for his edit and advice for the manuscript.

2.8. References

Baethgen, W.E., and Alley, M.M., 1989, A manual colorimetric procedure for measuring ammonium nitrogen in soil and plant Kjeldahl digests: Communications in Soil Science and Plant Analysis, v. 20, p. 961–969.

Banwart, W.L., Tabatabai, M.A., and Bremner, J.M., 1972, Determination of ammonium in soil extracts and water samples by an ammonia electrode: Communications in soil science and plant analysis, v. 3, p. 449–458.

Barnett, P.J., Sharpe, D.R., Russell, H.A.J., Brennand, T.A., Gorrell, G., Kenny, F., and Pugin, A., 1998, On the origin of the Oak Ridges Moraine: Canadian Journal of Earth Sciences, v. 35, p. 1152–1167.

Bedard-Haughn, A., Van Groenigen, J.W., and van Kessel, C., 2003, Tracing 15N through landscapes: potential uses and precautions: Journal of Hydrology, v. 272, p. 175–190.

Bower, C.E., and Holm-Hansen, T., 1980, A salicylate--hypochlorite method for determining ammonia in seawater: Canadian Journal of Fisheries and Aquatic Sciences, v. 37, p. 794–798.

Boyce, J.I., Eyles, N., and Pugin, A., 1995, Seismic reflection, borehole and outcrop geometry of Late Wisconsin tills at a proposed landfill near Toronto, Ontario: Canadian Journal of Earth Sciences, v. 32, p. 1331–1349.

Bradbury, K.R., Gotkowitz, M.B., Hart, D.J., Eaton, T.T., Cherry, J.A., Parker, B.L., and Borchardt, M.A., 2006, Contaminant transport through aquitards: technical guidance for aquitard assessment: Publication 91133b, American Water Works Association Research Foundation,.

Bremner, J.M., and Keeney, D.R., 1966, Determination and isotope-ratio analysis of different forms of nitrogen in soils: 3. exchangeable ammonium, nitrate, and nitrite by extraction-distillation methods 1: Soil Science Society of America Journal, v. 30, p. 577–582.

Brooks, P.D., Stark, J.M., McInteer, B.B., and Preston, T., 1989, Diffusion method to prepare soil extracts for automated nitrogen-15 analysis: Soil Science Society of America Journal, v. 53, p. 1707–1711.

Cacas, M.-C., Ledoux, E., de Marsily, G., Tillie, B., Barbreau, A., Durand, E., Feuga, B., and Peaudecerf, P., 1990, Modeling fracture flow with a stochastic discrete fracture network: calibration and validation: 1. The flow model: Water Resources Research, v. 26, p. 479–489.

Carpenter, K.D., Snyder, D.T., Duff, J.H., Triska, F.J., Lee, K.K., Avanzino, R.J., and Sobieszczyk, S., 2009, Hydrologic and water-quality conditions during restoration of the Wood River Wetland, Upper Klamath River basin, Oregon, 2003-05.:

Cavé, L., Al, T., Xiang, Y., and Vilks, P., 2009, A technique for estimating one-dimensional diffusion coefficients in low-permeability sedimentary rock using X-ray radiography: comparison with through-diffusion measurements: Journal of contaminant hydrology, v. 103, p. 1–12.

Celejewski, M., Barton, D., and Al, T., 2018, Measurement of Cl-: Br- Ratios in the Porewater of

Clay-Rich Rocks—A Comparison of the Crush-and-Leach and the Paper-Absorption Methods: Geofluids, v. 2018.

Celejewski, M., Scott, L., and Al, T., 2014, An absorption method for extraction and characterization of porewater from low-permeability rocks using cellulosic sheets: Applied geochemistry, v. 49, p. 22–30.

Chanton, J.P., and Whiting, G.J., 1996, Methane stable isotopic distributions as indicators of gas transport mechanisms in emergent aquatic plants: Aquatic Botany, v. 54, p. 227–236.

Cherry, J., 1990, Groundwater Monitoring: Some Deficiencies and Opportunities. Hazardous Waste Site Investigationns; Towards Better decision: Proceedings of 10th ORNL Life sciences symposium Gatlinberg, TN,.

Cherry, J.A., Parker, B.L., Bradbury, K.R., Eaton, T.T., Gotkowitz, M.B., Hart, D.J., and Borchardt, M.A., 2006, Contaminant transport through aquitards: a state-of-the-science review: Denver, Colorado: American Water Works Association Research Foundation,.

Cherry, J.A., Parker, B.L., Bradbury, K.R., Eaton, T.T., Gotkowitz, M.G., Hart, D.J., and Borchardt, M.A., 2004, Role of aquitards in the protection of aquifers from contamination: a “state of the science” report: Awwa Research Foundation, Denver, Colo,.

Clark, I., 2015, Groundwater geochemistry and isotopes: CRC press.

Clark, I.D., Al, T., Jensen, M., Kennell, L., Mazurek, M., Mohapatra, R., and Raven, K.G., 2013, Paleozoic-aged brine and authigenic helium preserved in an Ordovician shale aquiclude: Geology, v. 41, p. 951–954.

Crann, C.A., Murseli, S., St-Jean, G., Zhao, X., Clark, I.D., and Kieser, W.E., 2017, First status report on radiocarbon sample preparation techniques at the AE Lalonde AMS Laboratory (Ottawa, Canada): Radiocarbon, v. 59, p. 695–704.

Criss, R.E., 1999, Principles of stable isotope distribution: Oxford University Press on Demand.

Desaulniers, D.E., and Cherry, J.A., 1989, Origin and movement of groundwater and major ions in a thick deposit of Champlain Sea clay near Montreal: Canadian Geotechnical Journal, v. 26, p. 80–89.

Desaulniers, D.E., Cherry, J.A., and Fritz, P., 1981, Origin, age and movement of pore water in argillaceous Quaternary deposits at four sites in southwestern Ontario: Journal of Hydrology, v. 50, p. 231–257.

Desaulniers, D.E., Kaufmann, R.S., Cherry, J.A., and Bentley, H.W., 1986, 37Cl-35Cl variations in a diffusion-controlled groundwater system: Geochimica et Cosmochimica Acta, v. 50, p. 1757–1764.

Du, Y., Ma, T., Deng, Y., Shen, S., and Lu, Z., 2017, Sources and fate of high levels of ammonium in surface water and shallow groundwater of the Jianghan Plain, Central China: Environmental Science: Processes & Impacts, v. 19, p. 161–172.

Edwards, T.W.D., Wolfe, B.B., and Macdonald, G.M., 1996, Influence of changing atmospheric

circulation on precipitation $δ$ 18 O--temperature relations in Canada during the Holocene: Quaternary Research, v. 46, p. 211–218.

Eyles, N., and Clark, B.M., 1988, Last interglacial sediments of the Don Valley Brickyard, Toronto, Canada, and their paleoenvironmental significance: Canadian Journal of Earth Sciences, v. 25, p. 1108–1122.

Eyles, N., and Eyles, N., 2002, Ontario rocks: three billion years of environmental change: Fitzhenry & Whiteside Ltd.

Gerber, R., 1999, Hydrogeologic behaviour of the Northern till aquitard near Toronto, Ontario: National Library of Canada= Bibliothèque nationale du Canada.

Gerber, R.E., and Howard, K.W.F., 1996, Evidence for recent groundwater flow through Late Wisconsinan till near Toronto, Ontario: Canadian Geotechnical Journal, v. 33, p. 538–555.

Gerber, R.E., and Howard, K., 2000, Recharge through a regional till aquitard: Three-dimensional flow model water balance approach: Groundwater, v. 38, p. 410–422.

Hendry, M.J., 1988, Hydrogeology of clay till in a prairie region of Canada: Groundwater, v. 26, p. 607–614.

Hendry, M.J., Kelln, C.J., Wassenaar, L.I., and Shaw, J., 2004, Characterizing the hydrogeology of a complex clay-rich aquitard system using detailed vertical profiles of the stable isotopes of water: Journal of Hydrology, v. 293, p. 47–56.

Hendry, M.J., and Wassenaar, L.I., 1999, Implications of the distribution of $δ$D in pore waters for groundwater flow and the timing of geologic events in a thick aquitard system: Water Resources Research, v. 35, p. 1751–1760.

Hoefs, J., 2009, Stable isotope geochemistry: Springer, v. 285.

Huling, S.G., and Weaver, J.W., 1991, Ground water issue: dense nonaqueous phase liquids: US Environmental Protection Agency.

IAEA.database, 2019, Global Network of Isotopes in Percipitation (GNIP):

Jiao, J.J., Wang, Y., Cherry, J.A., Wang, X., Zhi, B., Du, H., and Wen, D., 2010, Abnormally high ammonium of natural origin in a coastal aquifer-aquitard system in the Pearl River Delta, China: Environmental science & technology, v. 44, p. 7470–7475.

Kassenaar, J.D.C., and Wexler, E.J., 2006, Groundwater modelling of the Oak Ridges Moraine area: CAMC-YPDT Technical Report,.

Kendall, C., and Aravena, R., 2000, Nitrate isotopes in groundwater systems, *in* Environmental tracers in subsurface hydrology, Springer, p. 261–297.

Kjarsgaard, B.A., Knight, R.D., Russell, H., Sharpe, D., Crow, H., and Olson, L., 2018, Newmarket Till Aquitard: Optimum grain packing, with a pore filling cement generates pseudo-concrete: Geological Survey of Canada, Current Research, v. Open file.

Knight, R.D., Stepner, D.A.J., Kjarsgaard, B.A., Sharpe, D.R., Crow, H., and Gerber, R., 2019, Lithology and geochemistry of a surficial sediment core,Pickering area, Southern Ontario: Geological Survey of Canada, Current Research, v. open File.

Koehler, G., Wassenaar, L.I., and Hendry, M.J., 2000, An automated technique for measuring $δ$D and $δ$18O values of porewater by direct CO2 and H2 equilibration: Analytical chemistry, v. 72, p. 5659–5664.

Li, L., Lollar, B.S., Li, H., Wortmann, U.G., and Lacrampe-Couloume, G., 2012, Ammonium stability and nitrogen isotope fractionations for NH4+--NH3 (aq)--NH3 (gas) systems at 20--70° C and pH of 2--13: applications to habitability and nitrogen cycling in low-temperature hydrothermal systems: Geochimica et Cosmochimica Acta, v. 84, p. 280–296.

Logan, C., Sharpe, D.R., and Russell, H.A., 2001, Regional three-dimensional stratigraphic modelling of the Oak Ridges Moraine area, southern Ontario: Natural Resources Canada, Geological Survey of Canada.

Midwood, A.J., and Boutton, T.W., 1998, Soil carbonate decomposition by acid has little effect on $δ$13C of organic matter: Soil biology and biochemistry, v. 30, p. 1301–1307.

Murseli, S., St-Jean, G., Hanna, D., and Clark, I., 2017, Method Development: Micro Vacuum-distillation Experiments (uVDE).:

O'Leary, M.H., 1988, Carbon isotopes in photosynthesis: Bioscience, v. 38, p. 328–336.

O'leary, M.H., Madhavan, S., and Paneth, P., 1992, Physical and chemical basis of carbon isotope fractionation in plants: Plant, Cell & Environment, v. 15, p. 1099–1104.

Remenda, V.H., Cherry, J.A., and Edwards, T.W.D., 1994, Isotopic composition of old ground water from Lake Agassiz: implications for late Pleistocene climate: Science, v. 266, p. 1975–1978.

Remenda, V.H., der Kamp, G., and Cherry, J.A., 1996, Use of vertical profiles of $δ$18O to constrain estimates of hydraulic conductivity in a thick, unfractured aquitard: Water Resources Research, v. 32, p. 2979–2987.

Roe, J.E., Anbar, A.D., and Barling, J., 2003, Nonbiological fractionation of Fe isotopes: evidence of an equilibrium isotope effect: Chemical Geology, v. 195, p. 69–85.

Roy, W.R., Glessner, J.J.G., Krapac, I.G., and Larson, T.H., 2003, Possible geological-geochemical sources of ammonium in groundwater: preliminary results, *in* Proceedings, 13th Annual Illinois Groundwater Consortium Symposium,.

Schwartz, F.W., Smith, L., and Crowe, A.S., 1983, A stochastic analysis of macroscopic dispersion in fractured media: Water Resources Research, v. 19, p. 1253–1265.

Sharpe, D.R., Barnett, P.J., Russell, H.A.J., Brennand, T.A., and Gorrell, G., 1999, Regional geological mapping of the Oak Ridges Moraine, Greater Toronto Area, southern Ontario: Current research, p. 123–136.

Sharpe, D.R., Dyke, L.D., Hinton, M.J., Pullan, S.E., Russell, H.A.J., Brennand, T.A., Barnett, P.J., and Pugin, A., 1996, Groundwater prospects in the Oak Ridges Moraine area, southern Ontario:

application of regional geological models: Current research, v. 1996, p. 181–190.

Sharpe, D.R., Pugin, A.J.-M., and Russell, H.A.J., 2018, Geological framework of the Laurentian trough aquifer system, southern Ontario: Canadian Journal of Earth Sciences, v. 55, p. 677–708.

Sharpe, D.R., and Russell, H.A.J., 2013, A revised hydrostratigraphic framework model of Halton Till in the Greater Toronto Area, Ontario: Geological Survey of Canada, Current Research, v. 11, p. 27.

Sharpe, D.R., Russell, H.A.J., and Logan, C., 2007, A 3-dimensional geological model of the Oak Ridges Moraine area, Ontario, Canada: Journal of Maps, v. 3, p. 239–253.

Sharpe, D.R., Russell, H.A.J., and Logan, C., 2002, Geological characterization of a regional aquitard: Newmarket Till, Oak Ridges Moraine area, southern Ontario, *in* Ground and Water: Theory to Practice: Proceedings of the 55th Canadian Geotechnical and 3rd joint IAH-CNC and CGS Groundwater Specialty Conferences, Niagara Falls, Ontario, October, p. 20–23.

Smith, D.B., Downing, R.A., Monkhouse, R.A., Otlet, R.L., and Pearson, F.J., 1976, The age of groundwater in the Chalk of the London Basin: Water Resources Research, v. 12, p. 392–404.

Smith, L., and Schwartz, F.W., 1984, An analysis of the influence of fracture geometry on mass transport in fractured media: Water Resources Research, v. 20, p. 1241–1252.

Toth, J., 1995, Hydraulic continuity in large sedimentary basins: Hydrogeology Journal, v. 3, p. 4–16.

Wang, X.-S., Jiao, J.J., Wang, Y., Cherry, J.A., Kuang, X., Liu, K., Lee, C., and Gong, Z., 2013, Accumulation and transport of ammonium in aquitards in the Pearl River Delta (China) in the last 10,000 years: conceptual and numerical models: Hydrogeology Journal, v. 21, p. 961–976.

Wassenaar, L.I., and Hendry, M.J., 1999, Improved piezometer construction and sampling techniques to determine pore water chemistry in aquitards: Groundwater, v. 37, p. 564–571.

Wexler, E., Holysh, S., Kassenaar, D., and Gerber, R., 2004, Regional and Sub-Regional Groundwater Flow Modelling, Oak Ridges Moraine Area of Southern Ontario.

Whiticar, M.J., 1999, Carbon and hydrogen isotope systematics of bacterial formation and oxidation of methane: Chemical Geology, v. 161, p. 291–314.

Yuan-Hui, L., and Gregory, S., 1974, Diffusion of ions in sea water and in deep-sea sediments: Geochimica et cosmochimica acta, v. 38, p. 703–714.

Chapter 3 – Conclusion

This study successfully demonstrated methods to use natural tracers in aquifer-aquitard systems to investigate mechanisms of solute transport. The combined evaluation of multiple datasets provides evidence that the Newmarket Till is an aquitard that effectively protects groundwater in the underlying aquifers. Key evidence includes the occurrence of what appears to be cold-climate water at depth in the system, low diffusion coefficients and lack of evidence for downward transport of NO_3^- and Cl^-, despite the downward hydraulic gradient.

The isotopic profiles of δ^2H and $\delta^{18}O$ in porewater and groundwater demonstrate the depletion trend versus depth meaning the porewater and groundwater in the Thorncliffe Formation originated from cold-climate conditions. Moreover, most of porewater samples have values similar to modern precipitation. On the other hand, the samples from the bottom of the borehole have the early – Holocene times signature. This suggests that the Newmarket impedes downward movement of modern precipitation into the lower part of the sequence.

The elevated concentrations of NO_3^- and Cl^- near the surface in comparison with the lower part, suggest that, due to low diffusion rates in the Newmarket Till, downward migration of anthropogenic contamination is inhibited, and we can conclude that the Newmarket Till acts as a protective, low-permeability barrier.

Organic matter in the reducing environment is a source for NH_4^+ via ammonification. Generally, mineralization of organic N does not cause isotopic fractionation, but fractionation between the organic source and the NH_4^+ is observed in this system. There are three possible explanations for this fractionation: (1) lighter isotopes diffuse faster than heavier ones, so the higher rate of diffusion can cause fractionation; (2) heavier isotopes prefer to partition to the exchange sites, causing fractionation along the transport path; (3) dissociation of NH_4^+ to NH_3 under anaerobic condition.

The high $\delta^{13}C$ ratio in the Thorncliffe Formation should be a result of equilibration with calcite and extensive methanogenesis. Biogenic CH_4 is produced in the system based on the stable isotope analysis of CH_4. During this process, the $\delta^{13}C$-DIC will be enriched because micro-organisms favor to select the lightest isotope of carbon (^{12}C). This also may help to explain the depleted trend for $\delta^{13}C$-DOC.

3.1. Future Recommendations

While the results of this study successfully demonstrate that the Newmarket Till is a low permeability unit and it can provide a protection for underlying aquifer. It also needs modeling to explain the transport of solute.

The following suggestions for future research directions:

a) The Newmarket Till is a regionally extensive, dense, stony, silty sand drumlinized diamicton. To assessing the integrity of aquitard, comparison with other samples from other boreholes will help identify the transport mechanisms.
b) Use other methods to extract porewater from sediment to prevent the limitation of crush and leach method (Dissolution of calcite). We extracted porewater with the paper absorption method, but this method needs some improvements.
c) Numerical modelling for ^{18}O and ^{2}H may provide additional information for transport mechanism in the 3-dimensional aquitard aquifer system.

Appendix A

A1.1. Porosity Measurements (Volumetric)

This section provides a summary of volumetric porosity measurements based on the analysis of samples collected in the October 2017 (Table A.1)

The simplest direct method to determine the pore volume of sample should be used a cylindrical core with known dimensions. The usual procedure is to determine the volume of water in the pores by using the heating method.

$M_{H_2O} = M_w - M_D$

where:

M_w is the total wet mass of the sample and M_D is the total dry mass of the sample. If we consider that the density of water is equal to 1 g cm^{-3} ($\rho_{H_2O} = 1$):

$M_{H_2O} = V_{H_2O}$

$V_p = V_T - V_s$

Porosity (φ) = $\frac{\text{Pore Volume}}{\text{Total Volume}} = \frac{V_p}{V_T}$

Bulk Density (ρ_{bulk}) = $\frac{M_D}{V_T}$

Where:

V_{H_2O} is the total volume of the water in the pores, V is the total volume of the sample, V_s is the solid volume, and V_p is the pore volumes.

Table A.1. Volumetric Porosity and Bulk density values for samples

No	Sample ID	Depth (mbgs)	Porosity (%)	Bulk Density (g/cm^3)
1	PD-PR-2.6	0.2	16.6	2.35
2	PD-PR-1.6	0.71	15.3	2.16
3	PD-PR-12.2	3.9	16.7	2.45
4	PD-PR-16.5	5.63	18.0	2.55
5	PD-PR-22.4	6.89	20.6	2.55
6	PD-PR-26.6	8.66	17.0	2.40
7	PD-PR-34.7	9.24	16.6	2.51
8	PD-PR-39.5	10.82	13.5	2.22
9	PD-PR-42.0	13.11	16.6	2.35
10	PD-PR-49.0	14.02	18.6	2.35
11	PD-PR-54.0	15.54	15.6	2.17
12	PD-PR-59.0	17.07	19.6	2.53
13	PD-PR-63.0	18.9	20.8	2.43
14	PD-PR-67.0	20.73	19.7	2.41
15	PD-PR-73.2	21.88	18.0	2.40
16	PD-PR-76.2	24.02	13.4	2.17
17	PD-PR-82.4	25.18	15.4	2.26
18	PD-PR-88.40	26.4	16.0	2.36
19	PD-PR-102.9	31.12	19.7	2.59
20	PD-PR-112.9	33.56	18.7	2.43
21	PD-PR-122.6	37.31	17.3	2.20
22	PD-PR-128.2	38.65	17.4	2.31
23	PD-PR-134.0	39.93	18.6	2.27
24	PD-PR-138.9	41.48	20.0	2.38
25	PD-PR-141.7	43.68	25.8	2.00
26	PD-PR-149.0	44.5	29.6	1.92
27	PD-PR-164.0	49.07	29.9	1.91
28	PD-PR-163.0	49.38	26.2	2.00
29	PD-PR-160.2	50.23	27.9	1.94

No	Sample ID	Depth (mbgs)	Porosity (%)	Bulk Density (g/cm^3)
30	PD-PR-169.6	50.41	29.6	2.22
31	PD-PR-168.2	50.84	27.1	2.22
32	PD-PR-173.8	52.18	34.7	2.04
33	PD-PR-179.4	53.52	35.6	1.99
34	PD-PR-178.2	53.89	38.3	2.03
35	PD-PR-176.6	54.38	37.9	1.95
36	PD-PR-182.7	55.57	27.3	1.93
37	PD-PR-189.1	56.66	30.6	2.31
38	PD-PR-193.3	58.53	30.3	2.31
39	PD-PR-198.3	59.95	35.4	1.99
40	PD-PR-201.5	62.03	31.3	2.13
41	PD-PR-207.8	63.15	33.8	2.17
42	PD-PR-213.1	64.59	30.7	1.94
43	PD-PR-217.0	66.45	44.3	1.92
44	PD-PR-224.2	67.5	32.9	2.18
45	PD-PR-222.8	67.73	39.7	2.02
46	PD-PR-229.5	68.73	38.4	1.86
47	PD-PR-228.5	69.04	42.9	2.04
48	PD-PR-226.4	69.68	39.0	1.98

A1.2. Porosity Measurements - Gravimetric

From ^{18}O and ^{2}H measurement process, we recorded the wet mass of sample before porewater extraction and the dry mass of the sample. So, we calculated the water content (w%):

$$w\% = \frac{M_{H_2O}}{M_T}$$

$$\frac{\varphi}{w} = \frac{M_T}{V_T} = \frac{M_S + M_{H_2O}}{V_T} = \rho_{bulk} + \varphi$$

$$\varphi = \frac{w \times \rho_{bulk}}{1-w}$$

where:

M_T is the total mass of the sample.

Table A1.2 displays the values of gravimetric measurements of porosity.

Table A.2. Water content, Gravimetric Porosity and Bulk density values for samples

NO	Sample ID	Depth (mbgs)	Water Content (%)	Bulk Density (g/cm3)	Porosity (%)
1	PD-OH-1.0	1.02	0.08	2.20	20
2	PD-OH-6.0	2.13	0.07	2.29	17
3	PD-OH-11.0	4.27	0.08	2.47	20
4	PD-OH-16.8	5.55	0.07	2.54	20
5	PD-OH-21.7	7.10	0.09	2.51	25
6	PD-OH-27.1	8.50	0.07	2.41	19
7	PD-OH-38.5	11.13	0.07	2.27	18
8	PD-OH-42.0	13.11	0.08	2.35	20
9	PD-OH-53.0	15.85	0.08	2.21	19
10	PD-OH-58.3	17.28	0.09	2.50	24
11	PD-OH-62.4	19.08	0.08	2.42	21
12	PD-OH-67.6	20.54	0.09	2.41	24
13	PD-OH-72.0	22.25	0.07	2.35	19
14	PD-OH-76.8	23.84	0.07	2.21	17
15	PD-OH-83.0	24.99	0.07	2.22	16
16	PD-OH-88.0	26.52	0.07	2.38	17
17	PD-OH-103.0	31.09	0.08	2.56	22
18	PD-OH-112.0	33.83	0.08	2.43	22
19	PD-OH-122.0	37.49	0.09	2.21	21
20	PD-OH-128.5	38.56	0.08	2.30	20
21	PD-OH-132.8	40.29	0.08	2.29	21
22	PD-OH-139.7	41.24	0.08	2.36	21
23	PD-OH-142.3	43.49	0.13	2.05	32
24	PD-OH-148.0	44.81	0.14	1.92	32
25	PD-OH-183.0	55.47	0.10	1.95	21
26	PD-OH-188.5	56.85	0.16	2.30	44
27	PD-OH-192.8	58.58	0.13	2.30	35
28	PD-OH-197.7	60.14	0.15	2.04	36
29	PD-OH-200.8	62.24	0.12	2.15	31
30	PD-OH-207.0	63.40	0.15	2.13	38

NO	Sample ID	Depth (mbgs)	Water Content (%)	Bulk Density (g/cm3)	Porosity (%)
31	PD-OH-212.5	64.77	0.17	1.94	38

A1.3. Crush and Leach Method

A1.3.1. Selection of Solid Liquid ratio (S/L) and Time Extraction

To test for the optimal S/L, we selected 9 samples. Water content was measured on these samples previously. To have a reliable estimation, from each part of the borehole (top, middle and bottom) three samples were picked up. Three S/L ratios selected for the analysis (1: 0.5, 1: 1, 1: 2) and then by comparing the results, the optimum one selected (Fig A.1 and Table A.3)

In order to find the minimum leaching time (this time includes centrifugation and filtration) for the crush and leach process, different time leaching was used for one sample (15min, 1hr, 3hr, 12hr). Figure A.2 and Table A.4 show the maximum concentration of elements occurred at 15 minutes. This is because by increasing the time most of the elements will go to the exchange sites.

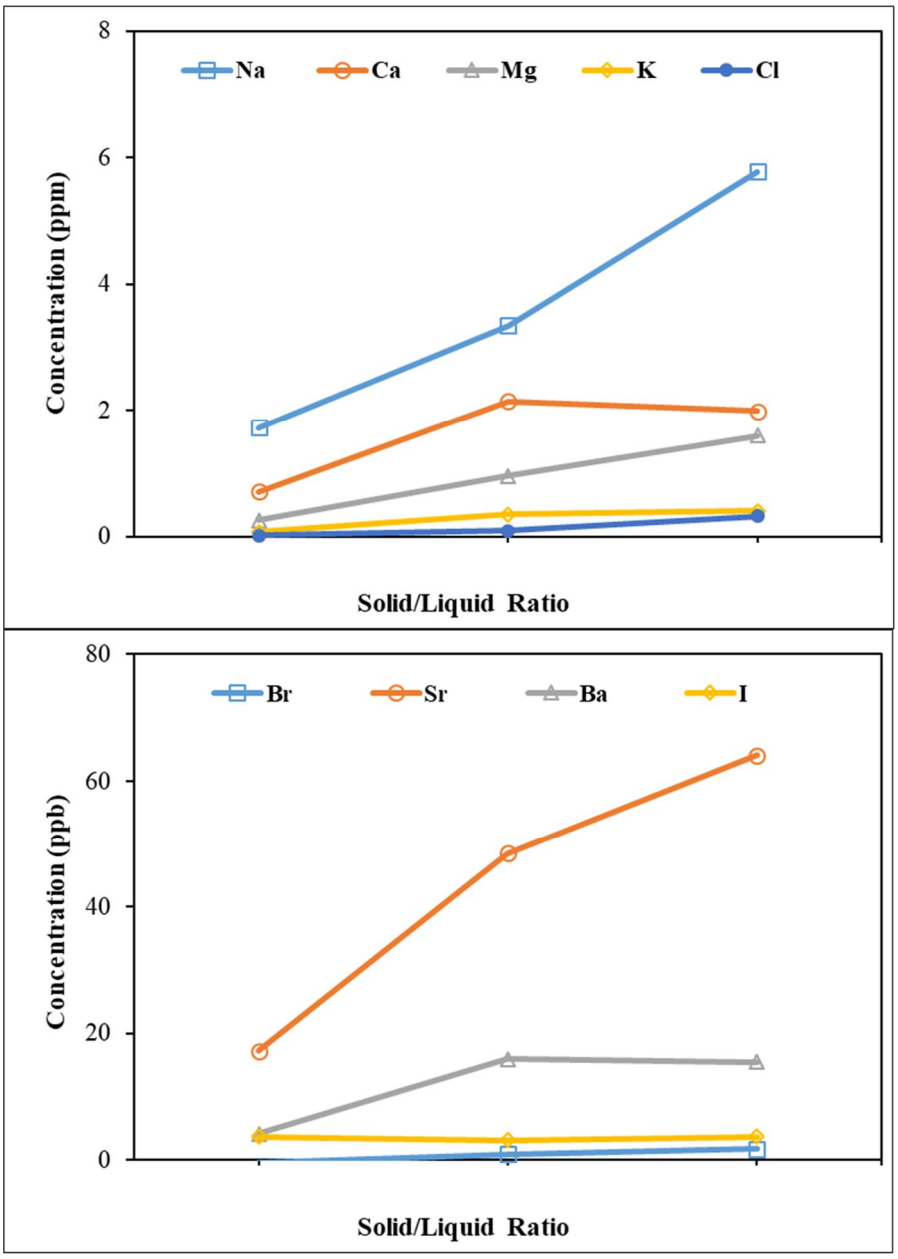

Fig. A.1. Compare concentration of the samples by using different S/L ratio (0.5, 1, 2)

Table A.3. Concentration of a sample using different S/L for crush and leach method

No	Sample ID	S/L Ratio	Time of Extraction (min)	Na (ppm)	Ca (ppm)	Mg (ppm)	Cl (ppm)	K (ppm)	Br (ppb)	Sr (ppb)	Ba (ppb)	I (ppb)
1	PD-PR-112.9	1:0.5	20	7.05	1.71	0.96	0.11	0.36	1.72	59.55	11.43	3.37
2	PD-PR-173.8	1:0.5	20	8.67	1.76	0.67	0.69	0.24	2.72	27.75	11.89	4.34
3	PD-PR-22.4	1:0.5	20	1.59	2.50	3.14	0.15	0.62	0.70	104.93	22.98	3.37
4	**S/L (2)**	**1:2**	**20**	**5.77**	**1.99**	**1.59**	**0.32**	**0.41**	**1.71**	**64.08**	**15.43**	**3.69**
5	PD-PR-201.5	1:1	20	3.17	3.67	1.36	-0.05	0.49	3.08	54.01	31.42	3.32
6	PD-PR-49.0	1:1	20	3.13	1.13	0.69	0.10	0.26	-1.07	43.39	6.13	3.07
7	PD-PR-138.9	1:1	20	3.74	1.63	0.80	0.22	0.28	0.77	48.12	10.34	2.96
8	**S/L (1)**	**1:1**	**20**	**3.35**	**2.14**	**0.95**	**0.09**	**0.34**	**0.93**	**48.51**	**15.96**	**3.12**
9	PD-PR-73.2	1:2	20	2.27	0.97	0.49	-0.01	0.19	-0.57	30.89	4.75	3.01
10	PD-PR-163	1:2	20	1.16	0.54	0.15	0.16	-0.01	-1.34	8.95	4.01	3.29
11	PD-PR-229.5	1:2	20	1.73	0.60	0.14	-0.11	0.04	0.61	11.82	3.68	4.51
12	**S/L (0.5)**	**1:2**	**20**	**1.72**	**0.71**	**0.26**	**0.01**	**0.07**	**-0.43**	**17.22**	**4.15**	**3.61**

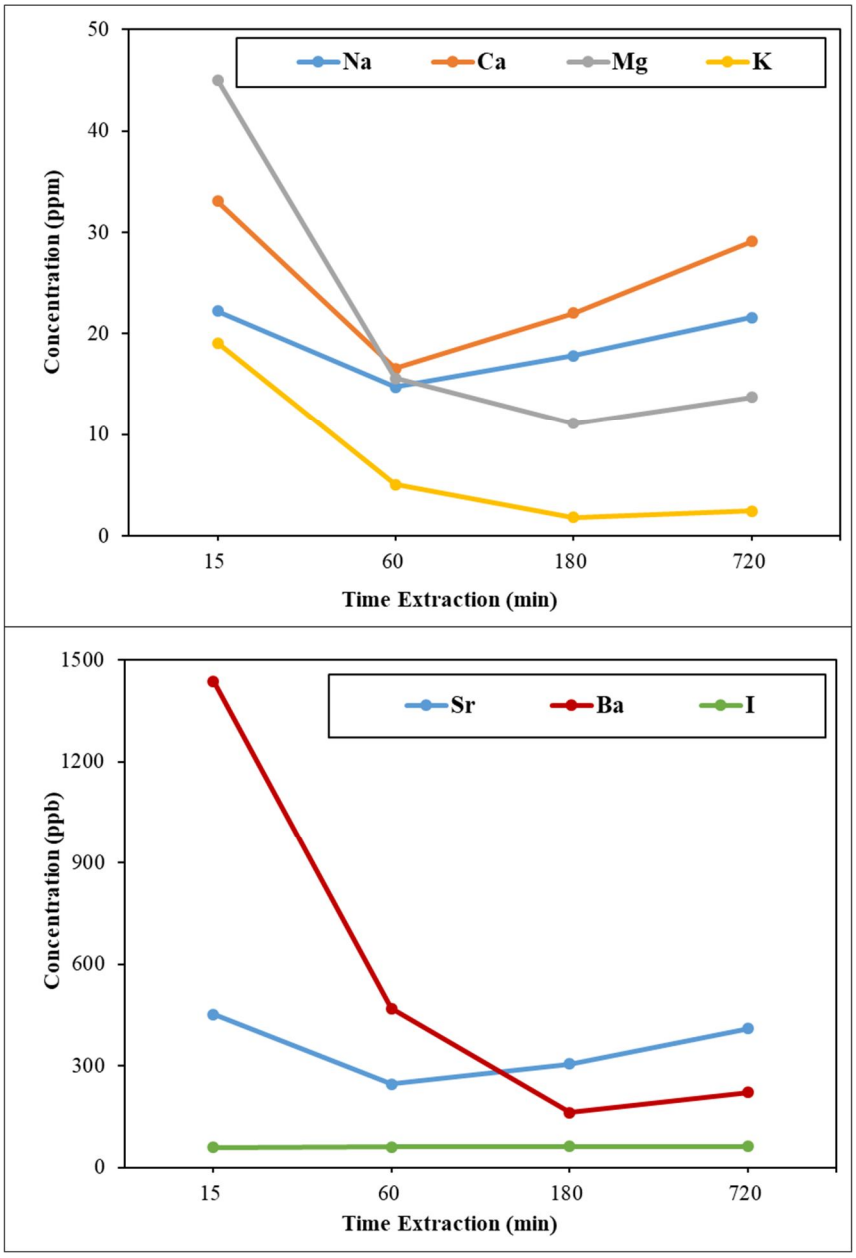

Fig. A.2. Compare concentration of the sample by using different time extraction (15, 50, 180, and 720 min)

Table A.4. Concentration of a sample using different time extraction for crush and leach method

No	Sample ID	S/L Ratio	Time of Extraction (min)	Na (ppm)	Ca (ppm)	Mg (ppm)	Cl (ppm)	K (ppm)	Br (ppb)	Sr (ppb)	Ba (ppb)	I (ppb)
1	C & L (0.25 hr) #1	1:2	15	22.52	35.75	48.53	1.43	20.76	3.28	488.88	1594.76	60.86
2	C & L (0.25 hr) #2	1:2	15	22.78	33.28	47.12	-2.31	20.47	-0.03	455.73	1459.99	58.40
3	C & L (0.25 hr) #3	1:2	15	21.40	30.19	39.50	-10.75	16.08	-12.83	411.57	1256.95	60.45
4	**C & L (0.25 hr)-Avg**	**1:2**	**15**	**22.23**	**33.07**	**45.05**	**-3.88**	**19.10**	**-3.19**	**452.06**	**1437.23**	**59.91**
5	C & L (1 hr) #1	1:2	60	16.80	15.28	8.04	1.19	1.25	-9.93	214.94	118.00	61.26
6	C & L (1 hr) #2	1:2	60	20.82	29.03	31.31	-7.53	12.39	-17.41	401.22	972.39	63.83
7	C & L (1 hr) #3	1:2	60	6.54	5.44	7.49	-18.56	1.50	-26.45	122.11	317.76	54.79
8	**C & L (1 hr)-Avg**	**1:2**	**60**	**14.72**	**16.58**	**15.61**	**-8.30**	**5.05**	**-17.93**	**246.09**	**469.38**	**59.96**
9	C & L (3 hr) #1	1:2	180	17.20	23.54	11.85	0.28	1.30	-19.19	329.35	149.36	63.41
10	C & L (3 hr) #2	1:2	180	17.79	21.54	10.46	-1.07	1.42	-12.84	301.73	147.21	63.54
11	C & L (3 hr) #3	1:2	180	18.46	21.07	10.89	0.40	2.69	-10.03	286.56	188.67	59.91
12	**C & L (3 hr)-Avg**	**1:2**	**180**	**17.81**	**22.05**	**11.07**	**-0.13**	**1.80**	**-14.02**	**305.88**	**161.75**	**62.28**
13	C & L (12 hr) #1	1:2	720	21.00	29.22	14.01	-9.03	2.21	-6.61	406.13	248.47	62.04
14	C & L (12 hr) #2	1:2	720	21.05	29.16	13.74	-1.64	2.30	-9.36	410.99	202.45	62.90
15	C & L (12 hr) #3	1:2	720	22.69	28.90	13.43	-3.21	2.77	-11.34	413.39	212.61	59.17
16	**C & L (12 hr)-Avg**	**1:2**	**720**	**21.58**	**29.09**	**13.73**	**-4.63**	**2.43**	**-9.11**	**410.17**	**221.18**	**61.37**

A1.3.2. Porewater Extraction (Crush and Leach)

The concentrations of cations and anions in porewater were determined by leaching the sediments (30 g) with 15 g of MilliQ water for 15 minutes. Phase separation was conducted by centrifugation and filtration (0.45 μm). Then the leachate samples were divided into two parts and prepared for anion analysis by Ion Chromatography (IC) (Table A. 5) and cation and anion analysis by Inductively Coupled Plasma Mass Spectrometry (ICP-MS) (Table A. 6).

Table A.5. Anion analysis of crush and leach samples by IC

NO	Sample ID	Depth (mbgs)	F (ppm)	Cl (ppm)	SO_4 (ppm)	NO_3 (ppm)
1	PD - Cl - 1.1	0.97	0.70	20.30	49.67	15.83
2	PD - Cl - 6.3	2.04	1.20	19.22	121.01	34.25
3	PD - Cl - 11.6	4.08	1.69	39.06	39.26	1.47
4	PD - Cl - 17.3	5.39	2.38	8.99	24.14	0.77
5	PD - Cl - 22.1	6.98	3.04	10.13	67.78	2.24
6	PD - Cl - 26.7	8.63	2.94	6.24	63.01	3.18
7	PD - Cl - 38.7	11.06	2.82	5.86	74.89	1.04
8	PD - Cl - 47.0	14.63	2.37	4.73	49.62	0.37
9	PD - Cl - 53.9	15.57	3.66	3.93	68.12	1.11
10	PD - Cl - 58.6	17.19	2.82	7.41	357.03	0.63
11	PD - Cl - 62.9	18.93	4.12	8.74	91.50	1.01
12	PD - Cl - 66.1	21.00	2.96	10.25	43.90	0.55
13	PD - Cl - 72.3	22.16	3.67	4.84	119.66	1.43
14	PD - Cl - 76.0	24.08	3.96	5.96	30.99	0.86
15	PD - Cl - 83.3	24.90	4.08	5.50	39.17	1.27
16	PD - Cl - 88.6	26.33	4.00	4.29	41.26	0.70
17	PD - Cl - 103.7	30.88	4.23	6.49	136.54	0.57
18	PD - Cl - 112.4	33.71	5.51	8.83	192.30	1.16
19	PD - Cl - 122.9	37.22	4.34	5.50	60.75	1.62
20	PD - Cl - 129.0	38.40	4.19	5.91	93.27	0.83

21	PD - Cl - 133.6	40.05	4.18	7.16	61.62	1.01
22	PD - Cl - 139.1	41.42	2.46	7.11	58.90	0.48
23	PD - Cl - 141.8	43.65	3.26	6.18	39.74	0.88
24	PD - Cl - 148.3	44.71	4.21	9.80	63.53	1.14
25	PD - Cl - 183.4	55.35	4.05	9.35	56.38	0.50
26	PD - Cl - 188.7	56.78	4.94	12.81	123.60	1.02
27	PD - Cl - 193.2	58.46	3.27	6.21	21.05	0.23
28	PD - Cl - 198.1	60.02	2.64	8.96	17.13	1.81
29	PD - Cl - 201.3	62.09	1.85	8.55	20.11	0.28
30	PD - Cl - 207.5	63.25	1.82	8.90	3.34	0.27
31	PD - Cl - 212.6	64.74	1.78	13.66	10.75	1.05

Table A.6. Anion and cation analysis of crush and leach samples by ICP-MS

NO	Sample ID	Depth (mbgs)	Na (ppm)	Mg (ppm)	Cl (ppm)	K (ppm)	Ca (ppm)	Mn (ppb)	Br (ppb)	Sr (ppb)	Ba (ppb)	I (ppb)
1	PD-CL-1.1	0.97	28.51	28.34	25.60	13.27	195.91	12.27	78.61	408.50	109.76	18.02
2	PD-CL-6.3	2.04	53.62	55.48	16.88	23.32	225.17	8.58	74.45	603.40	429.08	11.26
3	PD-CL-11.6	4.08	24.82	40.73	34.40	20.98	96.02	9.88	38.99	798.34	377.88	< LOD
4	PD-CL-17.3	5.39	41.76	31.76	8.06	14.95	42.26	9.92	37.03	802.35	186.27	4.65
5	PD-CL-22.1	6.98	39.42	42.04	5.79	14.02	43.50	8.83	28.15	1207.07	222.92	3.95
6	PD-CL-26.7	8.63	49.42	39.59	5.77	12.17	36.58	6.57	23.65	1249.46	178.11	5.80
7	PD-CL-38.7	11.06	109.96	9.40	3.13	8.73	17.74	12.94	30.39	466.29	75.43	23.51
8	PD-CL-47.0	14.63	206.23	15.51	8.45	10.21	43.74	32.01	42.45	851.33	111.49	30.31
9	PD-CL-53.9	15.57	147.61	6.18	7.75	6.01	22.53	21.52	35.05	349.70	48.64	15.63
10	PD-CL-58.6	17.19	118.22	4.79	7.63	4.38	21.25	23.69	25.65	279.73	40.12	13.44
11	PD-CL-62.9	18.93	144.73	3.42	2.82	5.20	13.52	21.13	41.68	185.19	44.56	14.92
12	PD-CL-66.1	21.00	132.86	4.26	4.71	4.99	18.32	41.22	47.69	198.98	63.81	14.71
13	PD-CL-72.3	22.16	173.18	2.69	3.16	6.09	11.64	26.52	51.44	147.00	52.60	29.54
14	PD-CL-76.0	24.08	188.61	5.18	4.97	6.60	20.43	25.31	62.54	296.17	57.29	19.73
15	PD-CL-83.3	24.90	165.50	4.15	5.59	7.31	16.03	65.58	53.01	146.83	110.98	21.26
16	PD-CL-88.6	26.33	170.42	3.86	7.18	6.56	15.88	52.80	76.89	169.86	92.43	33.79
17	PD-CL-103.7	30.88	167.62	3.35	5.96	4.82	16.14	25.40	64.11	212.57	41.27	24.74
18	PD-CL-112.4	33.71	120.39	2.60	6.22	4.25	11.78	27.89	56.16	140.26	45.53	15.44
19	PD-CL-122.9	37.22	127.53	2.47	6.34	3.83	11.69	17.33	58.95	146.59	29.43	21.91
20	PD-CL-129.0	38.40	164.20	2.92	6.58	4.55	14.41	25.19	129.68	174.83	40.51	54.69

21	PD-CL-133.6	40.05	117.83	3.00	4.24	4.03	12.15	16.17	64.99	170.48	32.28	23.97
22	PD-CL-139.1	41.42	110.33	3.31	5.79	4.52	13.46	25.36	69.93	183.56	44.03	31.65
23	PD-CL-141.8	43.65	105.28	6.22	7.50	5.10	17.25	15.73	151.16	314.37	174.43	21.51
24	PD-CL-148.3	44.71	82.96	4.03	6.77	3.00	11.88	17.87	105.40	192.83	67.54	20.11
25	PD-CL-183.4	55.35	70.29	23.34	8.51	10.09	65.70	35.12	99.15	667.79	371.77	18.83
26	PD-CL-188.7	56.78	69.48	20.23	8.09	7.71	55.52	27.89	99.65	557.07	289.51	13.92
27	PD-CL-193.2	58.46	79.92	25.81	7.82	8.96	71.10	41.33	116.15	721.67	383.09	11.57
28	PD-CL-198.1	60.02	66.74	17.71	6.60	6.27	46.06	21.26	94.33	493.29	287.35	20.49
29	PD-CL-201.3	62.09	78.57	20.32	9.99	9.40	55.71	32.62	129.61	611.55	347.06	569.15
30	PD-CL-207.5	63.25	66.04	18.75	7.00	7.94	54.56	33.87	96.68	583.71	290.66	113.84
31	PD-CL-212.6	64.74	49.96	14.12	5.50	6.73	44.49	36.53	88.14	472.23	218.15	22.91

For NH_4^+ measurements, 35 g of 2M KCl was used to extract total NH_4^+ in 3.5 g (wet mass) of sediment (Bremner and Keeney, 1966; Banwart et al., 1972). The mixture was immersed in an ultrasonic bath for 50 minutes and then phase separation was conducted by centrifugation (4200 rpm, 10 min) followed by filtration (0.45 μm nylon). The NH_4^+ concentrations in the extraction solutions were determined using the salicylate method (Bremner and Keeney, 1966; Bower and Holm-Hansen, 1980; Baethgen and Alley, 1989) with colorimetric measurements conducted with UV-VIS spectrophotometry (650 μm; Ocean Optics USB 4000) (Table A.7).

We measured the NH_4^+ in Tunney's Pasture samples. These samples got after two months; therefore, there were dried (Table A.8).

Table A.7. NH_4^+ concentrations in crush and leach samples

No	Sample ID	Depth (mbgs)	NH_4 Concentration (ppm)	Total Alkalinity as CaCO3 (mg/L)
1	PD - Cl - 1.1	0.97	4.05	676.62
2	PD - Cl - 6.3	2.04	6.37	866.09
3	PD - Cl - 11.6	4.08	42.41	499.73
4	PD - Cl - 17.3	5.39	69.86	366.59
5	PD - Cl - 22.1	6.98	55.98	402.32
6	PD - Cl - 26.7	8.63	60.23	445.60
7	PD - Cl - 38.7	11.06	70.48	410.31
8	PD - Cl - 47.0	14.63	53.89	336.80
9	PD - Cl - 53.9	15.57	45.52	334.26
10	PD - Cl - 58.6	17.19	44.92	308.06
11	PD - Cl - 62.9	18.93	56.90	366.21
12	PD - Cl - 66.1	21.00	43.01	414.84
13	PD - Cl - 72.3	22.16	79.83	497.98
14	PD - Cl - 76.0	24.08	81.31	439.47
15	PD - Cl - 83.3	24.90	12.72	528.97
16	PD - Cl - 88.6	26.33	40.81	512.38
17	PD - Cl - 103.7	30.88	40.51	592.57
18	PD - Cl - 112.4	33.71	34.58	389.63
19	PD - Cl - 122.9	37.22	35.26	415.25
20	PD - Cl - 129.0	38.40	43.72	434.21

21	PD - Cl - 133.6	40.05	54.87	402.60
22	PD - Cl - 139.1	41.42	60.30	379.20
23	PD - Cl - 141.8	43.65	85.59	330.57
24	PD - Cl - 148.3	44.71	175.32	274.40
25	PD - Cl - 183.4	55.35	304.74	561.09
26	PD - Cl - 188.7	56.78	396.21	478.00
27	PD - Cl - 193.2	58.46	343.31	583.42
28	PD - Cl - 198.1	60.02	427.46	416.05
29	PD - Cl - 201.3	62.09	454.55	502.76
30	PD - Cl - 207.5	63.25	514.67	501.87
31	PD - Cl - 212.6	64.74	480.83	358.74

Table A.8. NH_4^+ concentrations in crush and leach samples (dry samples)

No	Sample ID	Depth (mbgs)	NH_4 Concentration (ppm)	Total Alkalinity as CaCO3 (mg/L)
1	PD - 0.00	0.00	1.32	114.40
2	PD -10.00	0.10	0.56	141.52
3	PD - 20.00	0.20	1.00	126.91
4	PD - 30.00	0.30	1.16	198.82
5	PD - 40.00	0.40	0.97	187.09
6	PD - 90.00	0.90	0.04	132.71
7	PD - 100.00	1.00	0.00	119.55
8	PD - 125.00	1.25	< 0.00	117.66
9	PD - 145.00	1.45	< 0.00	115.25
10	PD - 175.00	1.75	0.00	144.37
11	PD - 200.00	2.00	0.01	153.30
12	PD - 225.00	2.25	0.00	80.28
13	PD - 250.00	2.50	< 0.00	104.87
14	PD - 275.00	2.75	0.01	86.11
15	PD - 300.00	3.00	0.05	101.10
16	PD - 350.00	3.50	0.05	97.03
17	PD - 450.00	4.50	0.34	83.24
18	PD - 500.00	5.00	0.16	94.34
19	PD - 600.00	6.00	0.17	74.32
20	PD - 750.00	7.50	0.22	81.62

21	PD - 650.00	6.50	0.50	101.87
22	PD - 700.00	7.00	0.48	111.76
23	PD - 810.00	8.10	0.23	79.15
24	PD - 880.00	8.80	0.21	74.60
25	PD - 950.00	9.50	0.09	81.42
26	PD - 1000.00	10.00	0.04	76.41
27	PD - 1030.00	10.30	0.12	80.34
28	PD - 1100.00	11.00	0.28	82.17
29	PD - 1140.00	11.40	0.08	88.27
30	PD - 1200.00	12.00	0.37	110.20
31	PD - 1250.00	12.50	0.44	103.51
32	PD - 1300.00	13.00	0.47	105.57
33	PD - 1350.00	13.50	0.50	108.42
34	PD - 1400.00	14.00	0.30	133.34
35	PD - 1450.00	14.50	0.41	124.85
36	PD - 1500.00	15.00	0.35	122.38

A1.4. Stable isotopes of water (^{18}O and ^{2}H)

The vacuum distillation (VD) method includes heating the crushed rock under vacuum, conjunction of water with liquid nitrogen trap. To start the process, the core sample was unpacked. Approximately 12 g sample was placed in 50 mL pre-weighed Erlenmeyer flasks and mounted on to the heater side of the individual vapor-transfer line. A 12 mL Labco exetainer, with a septum cap was placed on the water recovery side of the line (Fig A.3).

Before heating, to freeze the samples the loaded sample flasks were submerged in liquid nitrogen and were individually evacuated to 30 mTorr. Also, in this step the exetainer and water vapour transfer line were evacuated. Therefore, the transfer line isolated from the vacuum pump and the liquid nitrogen bath should be removed from the rock flasks and the bottom 3 cm of the exetainer should be submerged in to the liquid nitrogen bath. Then, the four Erlenmeyer flasks were put into the insulated resistance oven and the temperature of the rock samples was slowly increased over a period of around half an hour to 115C°. We selected this temperature because we tested the range of 100 to 150 C° for one of our sample over a period of 4 hours and based on the $\delta^{18}O$ and $\delta^{2}H$ results, we decided to use this temperature (Table A.9).

Water vapour released from the rock will be diffused through the transfer line because of the pressure differences between two sides. Then, under static vacuum, the vapor will be trapped cryogenically in the Labco exetainer.

When the extraction time completed, the oven removed, and rock flasks detached from the line and allowed them to cool. In addition, the exetainers disconnected from the line and closed with a septum cap and allowed to warm to room temperature.

The results for $\delta^{18}O$ and $\delta^{2}H$ are presented in Table A.10.

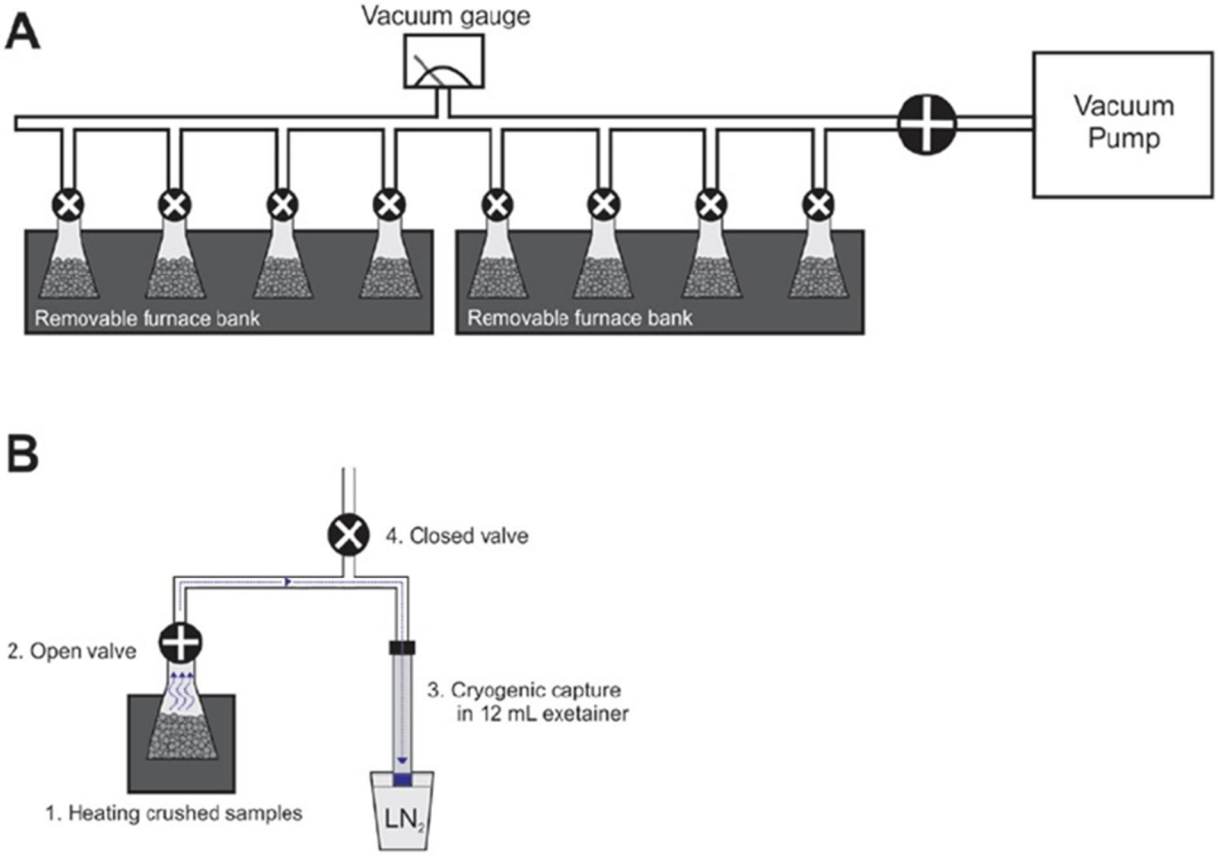

Fig. A.3. Vacuum distillation extraction line (VD), modified after (Murseli et al., 2017)

Table A.9. $\delta^{18}O$ and $\delta^{2}H$ results for porewater extraction using VD (selecting the temperature for heating)

No	Sample ID	Delta 2H (VSMOW)	Delta 18O (VSMOW)
1	PD-PP-123.3(1)- 150C	-77.95	-11.12
2	PD-PP-123.3(2)- 150C	-75.37	-10.93
3	PD-PP-123.3(3)- 150C	-74.05	-10.87
4	**Average (150 °C)**	**-75.79**	**-10.97**
5	PD-PP-123.3(1)- 115C	-74.20	-10.68
6	PD-PP-123.3(2)- 115C	-75.41	-10.84
7	PD-PP-123.3(2)- 115C	-75.75	-10.89
8	PD-PP-123.3(3)- 115C	-75.64	-10.98
9	**Average (115 °C)**	**-75.25**	**-10.85**

Table A.10. $\delta^{18}O$ and $\delta^{2}H$ results for porewater extraction using VD

No	Sample ID	Depth (mbgs)	Delta ^{2}H (VSMOW)	Delta ^{18}O (VSMOW)
1	PD-OH-1.0	1.02	-66.97	-9.62
2	PD-OH-6.0	2.13	-67.40	-9.74
3	PD-OH-11.0	4.27	-69.60	-10.08
4	PD-OH-16.8	5.55	-89.56	-12.55
5	PD-OH-21.7	7.10	-70.74	-9.83
6	PD-OH-27.1	8.50	-72.10	-10.14
7	PD-OH-38.5	11.13	-68.71	-9.88
8	PD-OH-42.0	13.11	-70.01	-10.25
9	PD-OH-53.0	15.85	-70.82	-10.56
10	PD-OH-58.3	17.28	-96.90	-13.65
11	PD-OH-62.4	19.08	-72.47	-10.55
12	PD-OH-67.6	20.54	-71.51	-10.24
13	PD-OH-72.0	22.25	-71.79	-10.11
14	PD-OH-76.8	23.84	-70.26	-10.23
15	PD-OH-83.0	24.99	-74.76	-10.71
16	PD-OH-88.0	26.52	-83.41	-12.20
17	PD-OH-103.0	31.09	-77.64	-11.31
18	PD-OH-112.0	33.83	-76.21	-10.83
19	PD-OH-122.0	37.49	-75.27	-10.35
20	PD-OH-128.5	38.56	-84.99	-12.65
21	PD-OH-132.8	40.29	-79.49	-11.95
22	PD-OH-139.7	41.24	-78.68	-11.13
23	PD-OH-142.3	43.49	-92.10	-13.34
24	PD-OH-148.0	44.81	-91.89	-13.41
25	PD-OH-183.0	55.47	-91.77	-12.41
26	PD-OH-188.5	56.85	-119.62	-15.85
27	PD-OH-192.8	58.58	-82.65	-10.98
28	PD-OH-197.7	60.14	-103.24	-14.22

No	Sample ID	Depth (mbgs)	Delta ^{2}H (VSMOW)	Delta ^{18}O (VSMOW)
29	PD-OH-200.8	62.24	-85.83	-11.38
30	PD-OH-207.0	63.40	-104.59	-14.40
31	PD-OH-212.5	64.77	-112.04	-15.97

A1.5. Paper Absorption Method to Extract Porewater

5 -10 mm of the outer core surface was removed. Then, split the sample and insert the 45mm diameter Whatman© 1 CHR paper directly in contact with the sample to extraction the porewater and solute by capillary and diffusion. The two segments were clamped together and enclosed in plastic wrap. Then, used the vinly tape to make sure that the paper was compressed between the sample. Finally, the sample vacuum-sealed in 2 poly bags (Fig A. 4).

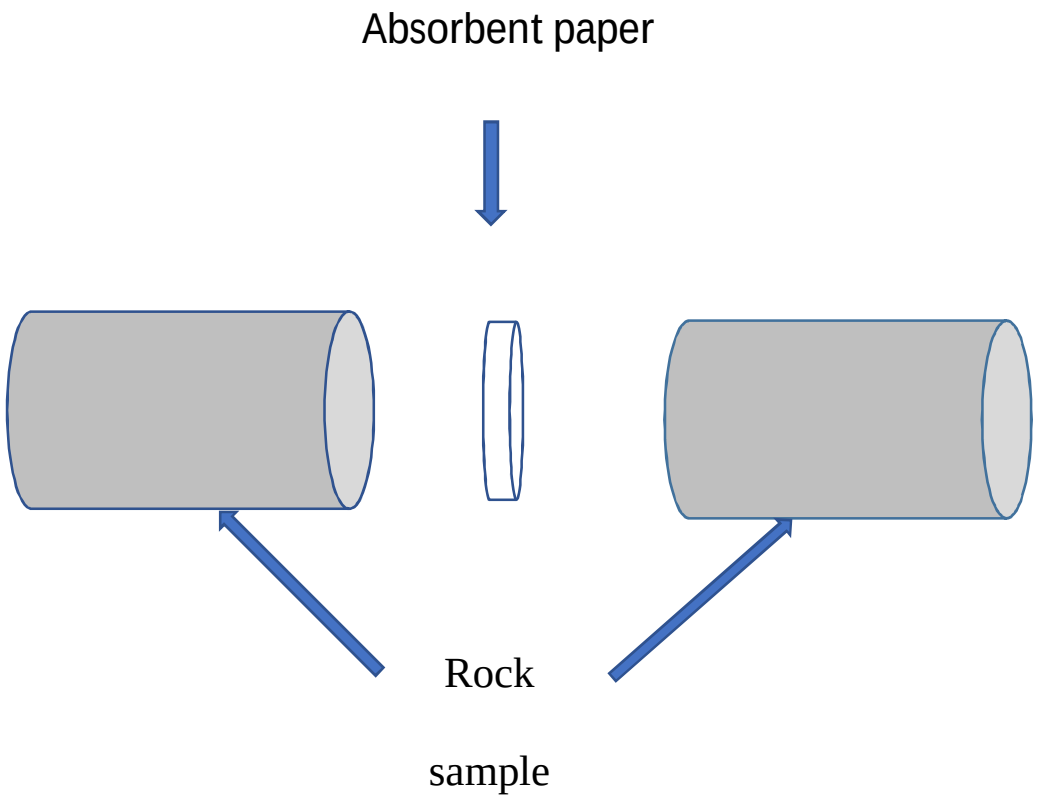

Fig. A.4. Schematic of the paper absorption method

This method is used to determine the possibility of porewater extraction by an absorbent material in direct contact by the core sample (Celejewski et al., 2014). After six weeks, the paper between the samples will be removed. The water-content will be measured by gravimetric and Near Infrared (NIR) spectrometry methods. We will use two type of sampling techniques in NIR. The transmission technique is used when the light is directed through the sample and then captured by the system. When the light onto the surface of the sample and then the reflected light is captured by the system, we use the reflection technique. Then, the papers will be leached for 24 hours with 10 mL of MilliQ water. Then the leachates will be filtered (0.45 μm) and prepared for IC and ICP-MS measurements.

The results for both IC and ICP-MS measurements are presented in Table A.11 and Table A.12.

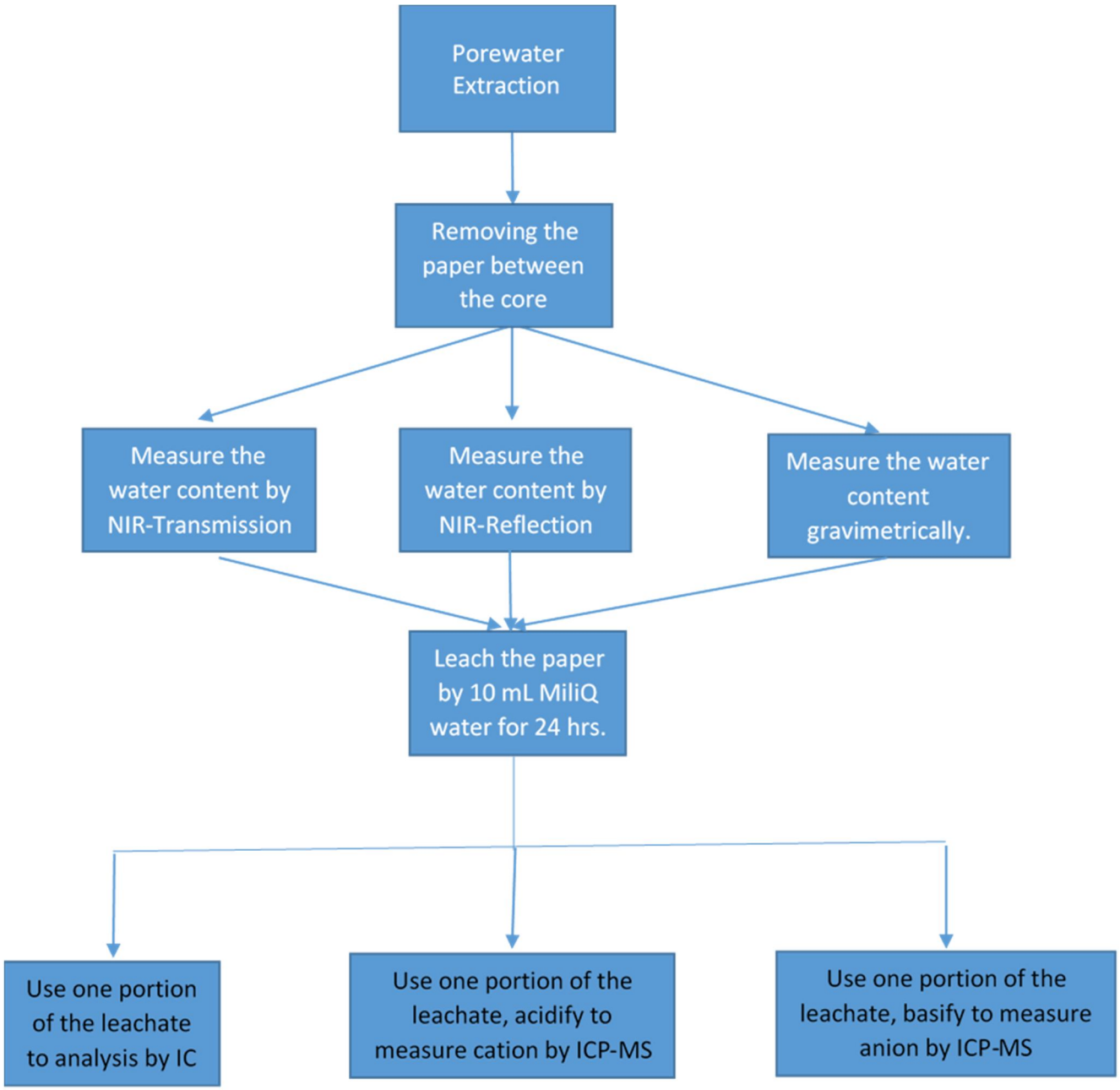

Fig. A.5. Process of porewater extraction with paper absorption method and the measurements

Table A.11. ICP-MS results for porewater measurements extracted by the paper absorption method

No	Sample ID	Depth (m)	Na (ppm)	Mg (ppm)	Cl (ppm)	K (ppm)	Ca (ppm)	Br (ppb)	Sr (ppb)	I (ppb)	Ba (ppb)
1	PD-PP-11.4	4.14	0.00	28.99	161.18	30.60	54.05	0.15	623.93	853.61	189.65
2	PD-PP-17.0	5.49	0.00	17.37	230.93	44.18	16.88	0.21	638.09	1555.84	92.82
3	PD-PP-21.9	7.04	0.00	46.16	125.86	26.01	138.28	0.18	1675.64	466.00	225.59
4	PD-PP-26.9	8.56	0.00	44.72	168.54	35.98	160.45	0.14	2015.49	652.81	263.61
5	PD-PP-39.0	10.97	0.00	27.79	188.02	35.28	234.44	0.16	1925.64	813.18	269.93
6	PD-PP-42.0	13.11	35.80	24.99	108.90	26.39	287.73	0.16	2309.78	572.73	313.18
7	PD-PP-47.0	14.63	8.84	21.81	92.22	29.33	259.31	0.17	2132.17	672.77	380.56
8	PD-PP-53.3	15.76	0.00	36.35	286.99	70.15	865.77	0.30	4581.07	1490.18	940.11
9	PD-PP-58.9	17.10	48.14	13.18	119.39	24.71	272.48	0.15	1608.09	545.53	189.70
10	PD-PP-62.6	19.02	28.61	12.73	148.49	29.97	195.86	0.21	1276.24	762.91	138.80
11	PD-PP-66.4	20.91	11.78	19.38	235.89	53.72	299.24	0.29	1980.31	1048.71	267.81
12	PD-PP-72.6	22.07	0.00	23.74	426.67	84.00	449.34	0.44	3113.10	1683.16	452.96
13	PD-PP-76.6	23.90	27.76	38.49	293.55	62.81	785.67	0.26	4576.64	1329.16	904.38
14	PD-PP-83.6	24.81	2.47	0.00	256.58	50.69	13.86	0.28	390.03	1731.86	126.20
15	PD-PP-82.8	25.05	28.96	22.84	101.39	25.79	352.74	0.16	2410.13	1033.70	457.58
16	PD-PP-82.6	25.12	0.00	0.00	279.10	55.10	0.00	0.42	90.10	1316.34	96.15
17	PD-PP-88.3	26.43	53.95	28.07	181.15	42.79	622.43	0.24	3349.20	1005.62	795.28
18	PD-PP-103.4	30.97	87.76	47.44	128.56	38.75	429.04	0.32	4125.95	762.42	517.20
19	PD-PP-112.8	33.59	60.62	10.03	96.34	19.23	217.75	0.19	1168.15	508.99	146.48
20	PD-PP-123.3	37.09	224.19	63.05	170.92	50.39	640.01	0.60	7197.68	1237.70	12516.64

21	PD-PP-128.8	38.47	11.87	0.00	180.06	32.53	0.00	0.26	79.65	887.62	13.62
22	PD-PP-133.8	39.99	0.00	0.00	255.13	47.33	0.00	0.30	19.26	1374.59	0.00
23	PD-PP-139.4	41.33	20.60	55.36	205.37	57.78	653.00	0.38	4685.07	1214.25	815.29
24	PD-PP-142.0	43.59	0.00	49.40	254.19	50.11	582.23	0.38	3344.87	1133.69	926.67
25	PD-PP-148.6	44.62	0.00	47.15	427.80	85.49	759.51	0.55	4577.04	2378.44	987.89
26	PD-PP-183.2	55.41	0.00	33.36	263.73	50.80	122.66	0.36	1232.40	1251.88	382.02
27	PD-PP-188.9	56.72	0.00	22.10	257.66	51.19	58.69	0.33	885.60	1552.32	229.89
28	PD-PP-193.0	58.52	0.00	19.72	166.60	32.50	52.80	0.23	678.79	848.78	204.12
29	PD-PP-197.1	60.32	0.00	20.34	451.92	88.69	62.04	0.44	952.79	1770.15	410.52
30	PD-PP-201.1	62.15	0.00	26.72	197.54	39.67	57.97	0.47	946.73	773.21	316.78
31	PD-PP-207.3	63.31	0.00	20.23	588.28	103.71	81.51	0.57	1099.88	3017.31	366.42
32	PD-PP-212.8	64.68	0.00	7.93	486.77	97.74	44.81	0.49	739.74	2802.26	340.20
33	PD-PP-231.8	71.08	0.00	2.11	507.56	105.24	37.57	1.81	1139.83	1794.08	938.25
34	PD-PP-231.6	71.14	0.00	0.00	587.08	117.20	15.29	2.16	753.81	3356.43	587.13
35	PD-PP-234.0	70.41	0.00	13.92	270.93	53.92	47.48	0.64	1147.42	1344.76	402.70

Table A.12. IC results for porewater measurements extracted by the paper absorption method

No	Sample ID	F (ppm)	Cl (ppm)	SO_4 (ppm)	Br (ppm)	NO_3 (ppm)	PO_4 (ppm)
1	PD-PP-11.4	0.56	0.78	0.23	0.02	0.09	0.01
2	PD-PP-17.0	0.42	0.21	0.09	0.01	0.06	n.d.
3	PD-PP-21.9	0.51	0.25	0.21	n.d.	0.04	n.d.
4	PD-PP-26.9	0.52	0.19	0.12	0.02	0.09	n.d.
5	PD-PP-39.0	0.50	0.56	0.34	0.02	0.05	n.d.
6	PD-PP-42.0	0.01	0.61	0.91	n.d.	0.08	0.02
7	PD-PP-47.0	0.40	0.37	0.30	n.d.	0.10	0.01
8	PD-PP-53.3	0.43	0.33	0.15	n.d.	0.08	0.02
9	PD-PP-58.9	0.48	0.29	0.81	n.d.	0.03	n.d.
10	PD-PP-62.6	0.44	0.25	0.51	n.d.	0.04	n.d.
11	PD-PP-66.4	0.48	0.28	1.21	0.02	0.12	0.01
12	PD-PP-72.6	0.50	0.11	0.13	0.02	0.07	n.d.
13	PD-PP-76.6	0.41	0.75	0.17	n.d.	0.09	0.01
14	PD-PP-83.6	0.39	0.18	0.71	0.02	0.09	n.d.
15	PD-PP-82.8	0.01	0.37	0.57	n.d.	0.06	0.02
16	PD-PP-82.6	0.44	0.16	0.25	0.02	0.09	0.02
17	PD-PP-88.3	0.38	0.24	2.04	n.d.	0.04	n.d.
18	PD-PP-103.4	0.01	0.33	1.63	n.d.	0.04	0.02
19	PD-PP-112.8	0.33	0.34	1.53	n.d.	0.05	n.d.
20	PD-PP-123.3	0.72	0.32	12.95	n.d.	n.d.	n.d.
21	PD-PP-128.8	0.35	0.23	0.63	0.02	34.81	n.d.
22	PD-PP-133.8	0.38	0.23	0.17	0.02	0.10	n.d.
23	PD-PP-139.4	0.41	0.25	0.10	n.d.	0.04	n.d.
24	PD-PP-142.0	0.45	0.17	1.86	0.03	0.05	n.d.
25	PD-PP-148.6	0.42	0.18	0.01	n.d.	0.05	n.d.
26	PD-PP-183.2	0.37	0.25	0.04	0.02	0.09	0.02
27	PD-PP-188.9	0.40	0.24	0.04	0.02	0.07	0.02
28	PD-PP-193.0	0.41	0.22	0.02	0.02	0.04	n.d.
29	PD-PP-197.1	0.51	0.09	0.01	0.02	0.05	n.d.
30	PD-PP-201.1	0.53	0.20	0.02	0.02	0.05	n.d.

No	Sample ID	F (ppm)	Cl (ppm)	SO_4 (ppm)	Br (ppm)	NO_3 (ppm)	PO_4 (ppm)
31	PD-PP-207.3	0.39	0.20	0.01	0.01	0.09	n.d.
32	PD-PP-212.8	0.38	0.14	0.01	0.01	0.06	0.01
33	PD-PP-231.8	0.49	0.50	0.05	0.02	0.09	0.01
34	PD-PP-231.6	0.39	0.50	0.03	0.02	0.07	n.d.
35	PD-PP-234.0	0.38	0.38	0.09	0.02	0.07	n.d.

A1.6. ^{15}N signature to Identify sources of NH_4^+

Generally, mineralization of organic N should not produce the fractionation. We measured ^{15}N in NH_4^+ and sediments to investigate the processes that caused fractionation in the system. The results are presented in Table A.13.

Table A.13. $\delta^{15}N$ in ammonium and sediment

No	Sample ID	$\delta^{15}N$-NH_4_Porewater (‰)	$\delta^{15}N$_Sediment (‰)
1	PD-CL-53.9	0.75	4.25
2	PD-CL-88.6	-1.40	4.56
3	PD-CL-133.6	3.65	4.92
4	PD-CL-183.4	6.81	3.96
5	PD - Cl - 188.7	…	4.23
6	PD-CL-193.2	7.14	3.80
7	PD-CL-198.1	6.38	4.48
8	PD-CL-201.3	8.01	4.37
9	PD - Cl - 207.5	…	4.25
10	PD-CL-212.6	6.64	4.17
11	Groundwater-Deep	0.99	…

A1. 7. Groundwater Results

For groundwater sampling, 3 PVC piezometers were installed in the borehole at the depths to the bottom of the screened interval (11.43 m, 50.31 m, and 70.12 m). Sample bottles were pre-cleaned with de-ionized water in the laboratory and in the field, the bottles were triple rinsed with sample water (pre-filtered as necessary) before the samples were collected. Water samples for dissolved organic carbon (DOC) and DIC were filtered using 0.45 μm filters (nylon) and stored at 4 °C in amber bottles.

Samples for dissolved methane (CH_4) were collected in a Wheaton bottle (1000 mL), acidified with 6N HCl (pH less than 2), and the bottles were sealed with a butyl septum without headspace. In the lab, CH_4 concentrations were measured by creating a headspace by gently displacing the water by high purity helium, typically 10% of the total bottle volume. The bottle is shaken for 5 minutes. The exsolved gases were analyzed by gas chromatography (GC) for N_2, O_2, CH_4, C_2H_6, C_3H_8, C_4H_{10}, and C_5H_{12}(SRI GC 8610C). For hydrogen and carbon isotopes in CH_4, the CH_4 was isolated by GC using a Poraplot Q column on a HP 7890A GC and isotopic measurements were made with a Delta-V Thermo IRMS interfaced to the GC.

Samples for ^{14}C analysis were collected in Wheaton amber glass bottle using prebaked (500 ˚C for 3 hours) 0.7 μm glass fiber filter (GF/F).

All the results presented in Table A.14.

Table A.14. Groundwater results for three piezometers

No	Groundwater samples	Depth (m)	$\delta^{2}H$ (‰)	$\delta^{18}O$ (‰)	DIC ppm	$\delta^{13}C$-DIC (‰)	DOC ppm	$\delta^{13}C$-DOC (‰)	CH_4 (ppm)	$\delta^{2}H$-CH_4 (‰)	$\delta^{13}C$-CH_4 (‰)	F14C_DIC
1	Shallow	11.43	-73.57	-11.02	37.66	-11.16	1.15	-27.88	0.07	N/A	-56.49	…
2	Intermediate	50.31	-78.15	-11.71	56.76	-7.56	3.96	-34.72	4.51	-278.57	-82.52	…
3	Deep	70.12	-77.62	-11.66	72.90	0.71	4.60	-33.63	10.52	-271.52	-77.47	0.13

A1.8. References

Baethgen, W.E., and Alley, M.M., 1989, A manual colorimetric procedure for measuring ammonium nitrogen in soil and plant Kjeldahl digests: Communications in Soil Science and Plant Analysis, v. 20, p. 961–969.

Banwart, W.L., Tabatabai, M.A., and Bremner, J.M., 1972, Determination of ammonium in soil extracts and water samples by an ammonia electrode: Communications in soil science and plant analysis, v. 3, p.449–458.

Bower, C.E., and Holm-Hansen, T., 1980, A salicylate--hypochlorite method for determining ammonia in seawater: Canadian Journal of Fisheries and Aquatic Sciences, v. 37, p. 794–798.

Bremner, J.M., and Keeney, D.R., 1966, Determination and isotope-ratio analysis of different forms of nitrogen in soils: 3. exchangeable ammonium, nitrate, and nitrite by extraction-distillation methods 1: Soil Science Society of America Journal, v. 30, p. 577–582.

Celejewski, M., Scott, L., and Al, T., 2014, An absorption method for extraction and characterization of porewater from low-permeability rocks using cellulosic sheets: Applied geochemistry, v. 49, p. 22–30.

Murseli, S., St-Jean, G., Hanna, D., and Clark, I., 2017, Method Development: Micro Vacuum-distillation Experiments (uVDE)